

Table 1
List of primers used in preparation of probe for *in situ* hybridization

Gene symbol	Gene product	Primer	Sequence
<i>Coll1a1</i>	Collagen, type XI, alpha 1	Sense	5'-TTT CCC AAA CTT GCA CAT'GA-3'
		Antisense	5'-CAC GCT GAG GAC AAT GAA GA-3'
<i>Sparcl1</i>	SPARC-like 1	Sense	5'-AAT GAA CTG GAC CAG CAT CC-3'
		Antisense	5'-AAA CGC AGA TGC ACA GAG TG-3'
<i>Tnn</i>	Tenascin-N	Sense	5'-CAA' GAC CTG GAA CAG GGT GT-3'
		Antisense	5'-TGC CTC TGT ATT TCC CAA CC-3'
<i>Coll15a1</i>	Collagen, type XV, alpha 1	Sense	5'-AAT CCG TAT CAG CCA CAA CC-3'
		Antisense	5'-TCC AGA ATC TTC CCT GTG CT-3'
<i>Hapln1</i>	Hyaluronan and proteoglycan link protein 1	Sense	5'-CAA GCA GAG AAG AGT CTG AG-3'
		Antisense	5'-GTT CTG CTT CCA CAA GTA GAC-3'
<i>Vit</i>	Vitrin	Sense	5'-CGA ATT TGG GTT CGA CAA GT-3'
		Antisense	5'-GAG CTC CTA GCC AGC CTT TT-3'
<i>Coll16a1</i>	Collagen, type XVI, alpha 1	Sense	5'-TAC CTC CAG GAT GCA GTT CC-3'
		Antisense	5'-TCC TGT AAG CTT TGG CCA TT-3'
<i>Smoc2</i>	SPARC related modular calcium binding 2	Sense	5'-ATC CAA GCC CAA AAA GTG TG-3'
		Antisense	5'-AGG GCA AGG GAA TAA ACC AG-3'
<i>Grn</i>	Grantulin	Sense	5'-ATG CTG TGT GCT GTG AGG AC-3'
		Antisense	5'-GTC CAC AGA AAC CGG AAG AA-3'
<i>Fbln5</i>	Fibulin 5	Sense	5'-AGG GGC GAC TAC CAT TTC TT-3'
		Antisense	5'-TGC GGC TAC CAC ACT AAT GA-3'
<i>Spon1</i>	Spondin 1	Sense	5'-AGA CGG TCT ACT GGG CAC TG-3'
		Antisense	5'-TGC AAA AGG ATG TGG TGG TA-3'
<i>Nid1</i>	Nidogen 1	Sense	5'-ACG TCA TGG GAA TCT TCA GC-3'
		Antisense	5'-TGC AAA CCG AAC TTC TGA TG-3'
<i>Leprel</i>	Leprecan 1	Sense	5'-GTC ACA GGC TGA GAG GAA GG-3'
		Antisense	5'-GCC CAG AGA AGA GTG TGT CC-3'
<i>TNN</i>	Human tenascin-N	Sense	5'-AAG ACC AGA GGT TTG CGT TG-3'
		Antisense	5'-GCT TAT ACC GCT CCT TGC TG-3'

periodontium lineage including PDL-progenitors. Differentiation of PDL-progenitors is initiated in the tooth root-forming stage of the tooth germ, and PDL formation is completed when the tooth erupts. Thus, DF provides a useful experimental model to

investigate the differentiation mechanisms of PDL (Yokoi et al., 2007). However, the precise differentiation mechanism of DF remains to be determined as the specific marker that distinguishes DF and PDL is not available. Therefore, it is important to identify the PDL cell lineage-specific markers to clarify the mechanism of DF cell differentiation.

The phenotypic property of a cell is determined by the unique combination of the expressed gene products. Therefore, the gene expression profile provides an informative modality to define the cellular marker of each tissue. The recent availability of genomic sequence information and high-throughput advances allow transcriptional analysis of highly specified organs such as PDL. Expressed sequence tags (ESTs) are short single-pass sequence reads of randomly selected clones from cDNA library, and they are invaluable for identification of genes and gene expression pattern in a particular type of tissue (Venter et al., 2003). Thus, an EST database could provide a platform for identification of PDL-specific markers. Here, we established the EST database for human PDL and examined the spatial and temporal expression patterns of 13 representative ESTs during PDL development.

2. Methods

2.1. Construction of human PDL cDNA library

The human PDL cDNA library was constructed using Plasmid System with Gateway Technology for Complementary DNA (cDNA) Synthesis and Cloning, as described in the manufacturer's protocols. After obtaining informed consent and approval (approval number 18) of the Ethics Committee of Kanagawa Dental College, PDL from extracted third molars were harvested. Total RNA was extracted using ISOGEN (Nippon Gene Co., Ltd, Tokyo, Japan) from PDL tissue and poly(A)⁺ mRNA was obtained with μ MACS mRNA Isolation Kit (Miltenyi Biotec Inc. Auburn, CA, USA), by following the manufacturer's protocols. cDNA was synthesized from poly(A)⁺ RNA with oligo dT primer using SuperScript Choice System (Invitrogen Corporation, Carlsbad, CA, USA), according to the manufacturer's instructions. The synthesized cDNA was separated based on size, and fractions > 1 kbp were inserted into the *SalI/NotI* restriction site of pBluescriptSK(-) plasmid (Stratagene, La Jolla, CA, USA). The ligated DNA was electroporated into competent *E. coli* cells (DH10B) by using E-coli Pulser (Bio-Rad Hercules, CA, USA).

2.2. DNA Sequencing and sequence data analysis

The plasmid DNA in transformed *E. coli* was amplified directly using TempliPhi DNA amplification kit (GE Healthcare, Piscataway, NJ, USA), and then cycle sequencing reactions were performed using M13 primer and Big Dye (v3.1). These were subjected to a 3730 DNA analyzer (Applied Biosystems, Foster City, CA, USA). A total of 11,520 clones from human PDL library were sequenced to obtain 5'EST. After trimming the vector sequence using the cross-match software, clustering of ESTs within a library was assembled by CAP3 sequence assembly program (Huang and Madan, 1999). To identify the gene

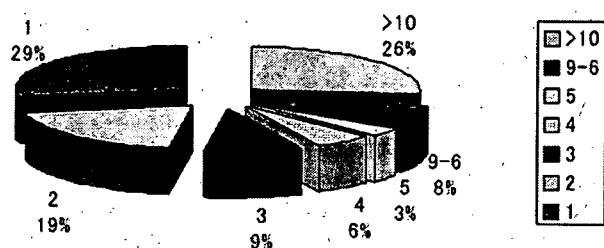


Fig. 1. Classification of ESTs according to their expression frequency. ESTs obtained by the sequencing analysis of human PDL cDNA library were classified according to their expression frequency (The number of same EST clones range from 1 to >10).

corresponding to each EST cluster, non-redundant clusters were analyzed against RefSeq data by BLAST (www.ncbi.nlm.nih.gov/BLAST). For the functional classification of each EST cluster, we used data of the gene ontology from GeneCards (<http://www.genecards.org/index.shtml>), Ensembl (<http://www.ensembl.org>), and GeneBank (<http://www.ncbi.nlm.nih.gov>).

2.3. Probes for *in situ* hybridization

The mouse homologues of the candidate EST clusters were searched from homologue (<http://www.ncbi.nlm.nih.gov/entrez/query.fcgi?db=homologue>). Specific primer for amplification of mouse cDNA is listed in Table 1. After amplification of cDNA by RT-PCR, the PCR product was subsequently cloned into pCR4 TOPO vector (Invitrogen Corporation, Carlsbad, CA, USA). The plasmid DNAs were linearized by *Not* I (antisense) or *Spe* I (sense) for *in situ* hybridization. The probe for periostin was used for control, as described previously (Yokoi et al., 2007).

2.4. *In situ* hybridization

To generate antisense and sense transcripts, digoxigenin-labeled riboprobes were prepared using T7 or T3 RNA polymerase, as described elsewhere (Wilkinson, 1995). Heads of

C57BL mice at embryonic (E) 13 days, E15, E17 and postnatal (P) 1 day were immediately frozen after embedding in OCT compound (Sakura Fine Technical Co., Ltd., Tokyo, Japan) and 10- μ m sagittal sections were made. Mandibles of 35-day postnatal mice were fixed in 4% paraformaldehyde at 4 °C overnight, decalcified with Morse's solution (Shibata et al., 2000) for 24 h, then embedded in OCT compound, and 10- μ m sagittal sections were made. *In situ* hybridization was carried out on these sections, as previously described with slight modification (Iseki et al., 1997). Polyvinyl alcohol was used as buffer during color reaction. Serial sections were made and *in situ* hybridization analysis was carried out 3 times per probe and stage.

2.5. *In vivo* differentiation assay

Human PDL cells (hPDL), a kind gift from Dr. T. Kawase (Approval number 8 from the Ethics Committee of Kanagawa Dental College), were cultured in α -minimum essential medium (α -MEM; Sigma, St. Louis, MO, USA) containing 10% fetal bovine serum (FBS; BioWhittaker, Maryland, USA), 50 μ g/ml of ascorbic acid, 100 units/ml of streptomycin and penicillin, in a humidified atmosphere of 5% CO₂ at 37 °C (Handa et al., 2002). Implantation of hPDL into SCID mice was carried out as described previously (Handa et al., 2002). Briefly, cells were inoculated subcutaneously into 5-week-old male CB-17 scid/scid (SCID) mice (Nihon Crea, Tokyo, Japan) after incubating 1.5×10^6 cells in a mixture of 40 mg of hydroxyapatite powder (Osferion; Olympus, Tokyo, Japan) and fibrin clot (mixture of mouse fibrinogen and thrombin; both from Sigma). Transplantation analysis was carried out 3 times, and 3 transplants were prepared per group. The mice were sacrificed after 4 weeks, and subjected to histochemical analysis with immunohistochemical staining or *in situ* hybridization as described below.

2.6. Histochemical analysis

The transplants were fixed in 4% paraformaldehyde for 1 day, decalcified with 12.5% EDTA containing 2.5% paraformaldehyde for 3 days and then embedded in OCT compound to produce frozen sections. Subsequently, 100 serial sections of 10- μ m thickness were made per implant, and analyzed histochemically. Expression of mRNA for *tenascin-N* was examined by *in situ* hybridization as described above. In immunohistochemical analysis, to avoid nonspecific staining of mouse monoclonal antibodies, sections were blocked using the M.O.M kit (Vector Laboratories, Burlingame, CA, USA). The sections were incubated with anti-vimentin monoclonal antibody (V9; Dako, Carpinteria, CA, USA) for 1 h. Dilutions were made with PBS containing 2 mg/ml bovine serum albumin. The sections were incubated with nonimmune mouse IgG, which served as a control. After washing, fluorescence was observed by fluorescence microscopy (Axio Imager; Carl Zeiss, Jena, Germany).

2.7. RNA preparation and real time PCR analysis

Total RNA was isolated from cells using ISOGEN (Nippon Gene Co., Ltd.), as described previously (Handa et al., 2002).

Table 2

Functional categorization of EST clusters in the KK-Periome database

1. Known function clusters	481 (78%)
(1) Ribosomal proteins	19 (3%)
(2) Initiation/elongation factors	9 (1%)
(3) Cell cycle	18 (3%)
(4) Energy production	45 (7%)
(5) Extracellular matrix proteins	39 (6%)
(6) Plasma membrane proteins	44 (7%)
(7) Signaling molecules	12 (2%)
(8) Proteinase	12 (2%)
(9) Intracellular signaling	96 (15%)
(10) Transcriptional factors	40 (6%)
(11) Cytoskeleton-related proteins	25 (4%)
(12) Other functions	122 (20%)
2. Unknown function clusters	101 (16%)
3. Unknown transcript clusters	35 (6%)
Total clusters	617 (100%)

After redundancy analysis, the clusters that showed an expression frequency of more than three times were collected and perform functional annotation. Parameters of functional categorization and proportion are shown.

Table 3
List of extracellular matrix ESTs expressed in the KK-Periome database

Frequency	Refseq ID	Gene symbol	Gene product	Reference
274	NM_000089	COL1A2	Collagen, type I, alpha 2	Lukinmaa et al. (1992)
156	NM_003118	SPARC	Secreted protein, acidic, cysteine-rich	Takano-Yamamoto et al. (1994)
133	NM_000090	COL3A1	Collagen, type III, alpha 1	Tsubota et al. (2002)
81	NM_006475	POSTN	Periostin	Kruzynska-Freitag et al. (2004)
65	NM_002345	LUM	Lumican	Hall et al. (1997)
62	NM_000088	COL1A1	Collagen, type I, alpha 1	Lukinmaa et al. (1992)
57	NM_000582	SPP1	Osteopontin	D'Errico et al. (1997)
43	NM_133506	DCN	Decorin	Matsuura et al. (2001)
24	NM_212482	FN1	Fibronectin	Hou et al. (1999)
21	NM_017680	ASPN	Asporin	Yamada et al. (2001)
19	NM_080645	COL12A1	Collagen, type XII, alpha 1	MacNeil, et al. (1998)
17	NM_000393	COL5A2	Collagen, type V, alpha 2	Lukinmaa and Waltimo (1992)
16	NM_014208	DSPP	Dentin sialophosphoprotein	D'Errico et al. (1997)
15	NM_057167	COL6A3	Collagen, type VI, alpha 3	Sloan et al. (1993)
*11	NM_080630	COL11A1	Collagen, type XI, alpha 1	
10	NM_004385	CSPG2	Versican	Shibata et al. (2002)
9	NM_002160	TNC	Tenascin C	Sahlberg et al. (2001)
8	NM_004967	IBSP	Bone sialoprotein	D'Errico et al. (1997)
8	NM_001711	BGN	Biglycan	Matsuura et al. (2001)
*6	NM_004684	SPARCL1	SPARC-like 1	
6	NM_000138	FBN1	Fibrillin 1	Sawada et al. (2006)
6	NM_005014	OMD	Osteomodulin	Petersson et al. (2003)
*6	NM_022093	TNN	Tenascin-N	
*5	NM_001855	COL15A1	Collagen, type XV, alpha 1	
*4	NM_001884	HAPLN1	Hyaluronan and proteoglycan link protein 1	
4	NM_004407	DMP1	Dentin matrix acidic phosphoprotein	Worapamorn et al. (2000)
*4	NM_053276	VIT	Vitrin	
4	NM_002290	LAMA4	Laminin, alpha 4	Salmivirta et al. (1997)
4	NM_006485	FBLN1	Fibulin 1	Sawada et al. (2006)
*4	NM_001856	COL16A1	Collagen, type XVI, alpha 1	
*3	NM_022138	SMOC2	SPARC related modular calcium binding 2	
*3	NM_002087	GRN	Granulin	
*3	NM_006329	FBLN5	Fibulin 5	
*3	NM_006108	SPON1	Spondin 1	
*3	NM_002508	NID1	Nidogen 1	
*3	NM_022356	LEPRE1	Leprecan 1	
3	NM_001849	COL6A2	Collagen, type VI, alpha 2	Sloan et al. (1993)
3	NM_000093	COL5A1	Collagen, type V, alpha 1	Lukinmaa and Waltimo (1992)

ESTs which are classified as an extracellular matrix, are listed according to frequency level.

Numbers given show the relative expression level of the ESTs. Asterisks show the gene clusters that have not been analyzed expression in the PDL.

cDNAs were synthesized from 1 µg of total RNA in a 20 µl reaction containing 10× reaction buffer, 1 mM dNTP mixture, 1 U/µl RNase inhibitor, 0.25 U/µl reverse transcriptase (M-MLV reverse transcriptase, (Invitrogen) and 0.125 µM random 9-mers (Takara, Tokyo, Japan). Normalization was performed using house keeping gene, glyceraldehyde-3-phosphate dehydrogenase (*GAPDH*) expression as an endogenous control in the same reaction as the gene of interest. The primers for real time PCR were designed with Primer 3 soft ware (http://frodo.wi.mit.edu/cgi-bin/primer3/primer3_www.cgi) based on the target gene. The details are; type XII collagen alpha1; sense 5'-GGA GAC AGA GGC TTC ACT GG -3', antisense 5'-TCC TTT CAA CCC AGA TGG AC-3', periostin; sense 5'-GAT GGA GTG CCT GTG GAA AT-3', antisense 5'-TGG TGA CCT TGG TGA CCT CT-3' antisense 5'-CCA AAG TTC CCA AGC TGA AC-3', F-spondin; sense 5'-ACT CCA CAT GGA GAG GCA AC -3', antisense 5'-AAG AGA TGG GCA AAC AAT GG-3'; tenascin-N; sense 5'-GCT CAG ATC CAC GGC TAC AT-3', antisense 5'-GAC CAC CCT TAA AGG CAA CA-

3' and glyceraldehyde-3-phosphate dehydrogenase (*GAPDH*): sense 5'-GTC AGT GGT GGA CCT GAC CT-3', antisense 5'-TCG CTG TTG AAG TCA GAG GA-3'. For real time PCR, the reaction was performed with *Power SYBR® Green PCR Master Mix* (Applied Biosystems), and products were analyzed with AB 7300 Real-Time PCR System (Applied Biosystems).

3. Results

3.1. Sequence analysis of ESTs from human PDL cDNA library

In order to analyze the expression profile in human PDL cDNA library, a total of 11,520 cDNA clones were randomly selected, and sequenced from the 5' ends. A total of 11,520 clones were sequenced from 5'ends, and 9600 high quality sequences were processed for further analysis. Redundancy analysis resulted in 4384 independent EST clusters. Expression frequency of each EST ranged from one to ten times or as high as 274 times (Fig. 1 and Table 3). We considered 617 EST

		<i>Coll1a1</i>	<i>Sparrcl1</i>	<i>Tnn</i>	<i>Coll15a1</i>	<i>Hapln1</i>	<i>Vit</i>	<i>Coll16a1</i>	<i>Smoc2</i>	<i>Grn</i>	<i>Fbln5</i>	<i>Spn1</i>	<i>Nid1</i>	<i>Leprel</i>
	expression frequency	11	6	6	6	4	4	4	3	3	3	3	3	3
P1	dental follicle		Gray	Black	Gray		Gray					Black		
	dental papilla		Gray						Black					
	odontoblast	Gray				Black		Gray		Gray			Gray	Black
	ameloblast									Gray	Gray			Gray
	alveolar bone	Black	Gray						Black					Gray
P35	periodontal ligament	Gray	Gray	Black	Gray	Gray		Black	Gray				Gray	Black
	cementoblast		Black										Gray	
	dental pulp		Gray							Gray				
	odontoblast	Black	Black			Gray		Black		Black				Black
	alveolar bone													

Fig. 2. *In situ* hybridization and expression frequency of 13 different ECMs in the developing tooth germ (P1) or adult periodontium (P35). *In situ* hybridization analysis of 13 ECM clusters in tooth germ at postnatal 1 day (P1) or adult periodontium (P35) are shown. ECM clusters are listed according to the expression frequency, type of cells in P1-tooth germ or P35-periodontium. Note that *F-spondin* (*Spn1*) is intensely expressed in the dental follicle cells. In contrast, *tenascin-N* (*Tnn*) is strongly expressed in the periodontal ligament. Black: strongly positive expression; Gray: weakly positive expression; White: No expression.

clusters with an expression frequency of more than 3 times as highly expressed genes in the PDL (Table 3).

3.2. Establishment of KK-Periome database

These 617 EST clusters were classified into 12 categories according to their ontology function (Table 2) (Yamada et al., 2001). Redundancy analysis identified 481 ESTs (78%) as known clusters, 101 ESTs (16%) as unknown function clusters and 35 ESTs (6%) as unknown transcript clusters, perhaps intra- and inter-genic transcripts. The largest category included secreting molecules such as ECMs, plasma membrane, proteases and protease inhibitors and signaling molecules (Table 2). The next abundant ESTs included genes involved in cellular signaling (such as ras homolog gene family member A, sorting nexin 17, and insulin-like growth factor binding protein 4), energy production (such as carboxypeptidase E, GNAS complex locus, ATP synthase H+ transporting, and mitochondrial F1 complex) and transcription factors (such as those similar to H3 histone family 3B, Y box binding protein 1, and HMT1 hnRNP methyltransferase-like 3).

3.3. Expression pattern of 13 extracellular matrix genes

We focused on ESTs for ECM in the KK-Periome database. As shown in Table 3, the top 10 transcripts were type I collagen alpha 2 (*COL1A2*), SPARC/osteonectin, collagen type III (*COL3A1*), periostin (*POSTN*), lumican (*LUM*), type I collagen alpha 2 chain (*COL1A1*), osteopontin (*SPP1*), decorin (*DCN*), fibronectin (*FNI*), and PLAP-1/Asporin (*ASPN*). These are major ECM components in PDL. The rest of ESTs include cementoblast/osteoblast markers such as bone sialoprotein (*IBSP*), osteomodulin (*OMD*) and dentin matrix acidic phosphoprotein 1 (*DMPI*) (D'Errico et al., 1997). To identify genes related to PDL formation, we screened the EST clusters, which are highly expressed during PDL development. For this purpose, the EST clusters which have been reported in PDL

were selected by PubMed search and 13 EST clusters were obtained as candidates including collagen type XI alpha 1 (*COL11A1*), SPARC-like 1 (*SPARCL1*), tenascin-N (*TNN*), collagen type XV alpha 1 (*COL15A1*), hyaluronan and proteoglycan link protein 1 (*HAPLN1*), vitrin (*VIT*), type XVI collagen alpha 1 (*COL16A1*), SPARC related modular calcium binding 2 (*SMOC2*), granulin (*GRN*), fibulin 5 (*FBLN5*), F-spondin (*SPON1*), nidogen 1 (*NID1*) and leprecan 1 (*LERPE1*).

The mouse ortholog of human candidate genes was selected, and subjected to *in situ* hybridization analysis to examine whether they were expressed in P1-DF or in P35-PDL. The results of the analysis were classified according to expression frequency, postnatal stage and type of cells in P1-tooth germ or P35-periodontium (Fig. 2). F-spondin was expressed specifically in P1-DF, and no expression was found in other cell types in the P1-tooth germ, suggesting that it could serve as a proper marker. Nidogen 1 was also intensely expressed in DF as well as odontoblasts. The remaining candidate genes showed weak or no expression in DF, while they were expressed in other cells of the tooth germ. In P35-PDL, the expression patterns of candidate genes were significantly different from those of P1-DF. Expression of F-spondin and nidogen 1 was markedly decreased in P35-PDL, whereas expression of tenascin-N, type VI collagen alpha 1, and leprecan was strikingly up-regulated. Among the up-regulated genes, tenascin-N was highly restricted to P35-PDL, indicating that it could serve as a marker for PDL.

3.4. Expression pattern of F-spondin and tenascin-N

To determine whether F-spondin and tenascin-N are involved in the formation of PDL, we examined the expression pattern of these genes during PDL development. F-spondin was initially expressed in E15-DF cells surrounding dental epithelium (Fig. 3Ab) and became progressively evident in the E17 and P1 DF cells (Fig. 3A, c and d). However, expression of F-spondin was significantly down-regulated in P7-DF cells, and no expression was detected in P35-PDL (Fig. 3B, a and b). In contrast, expression of tenascin-N

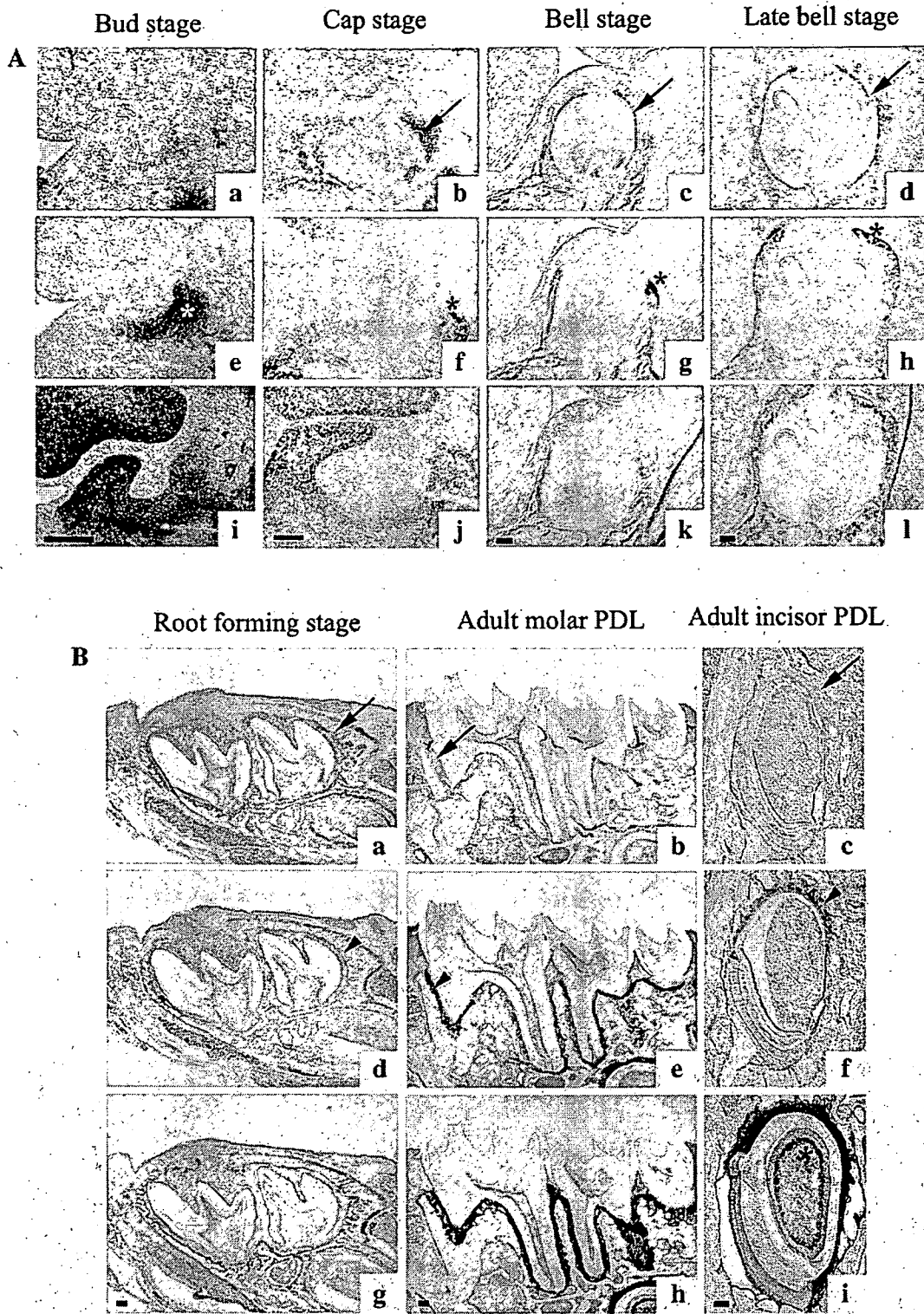
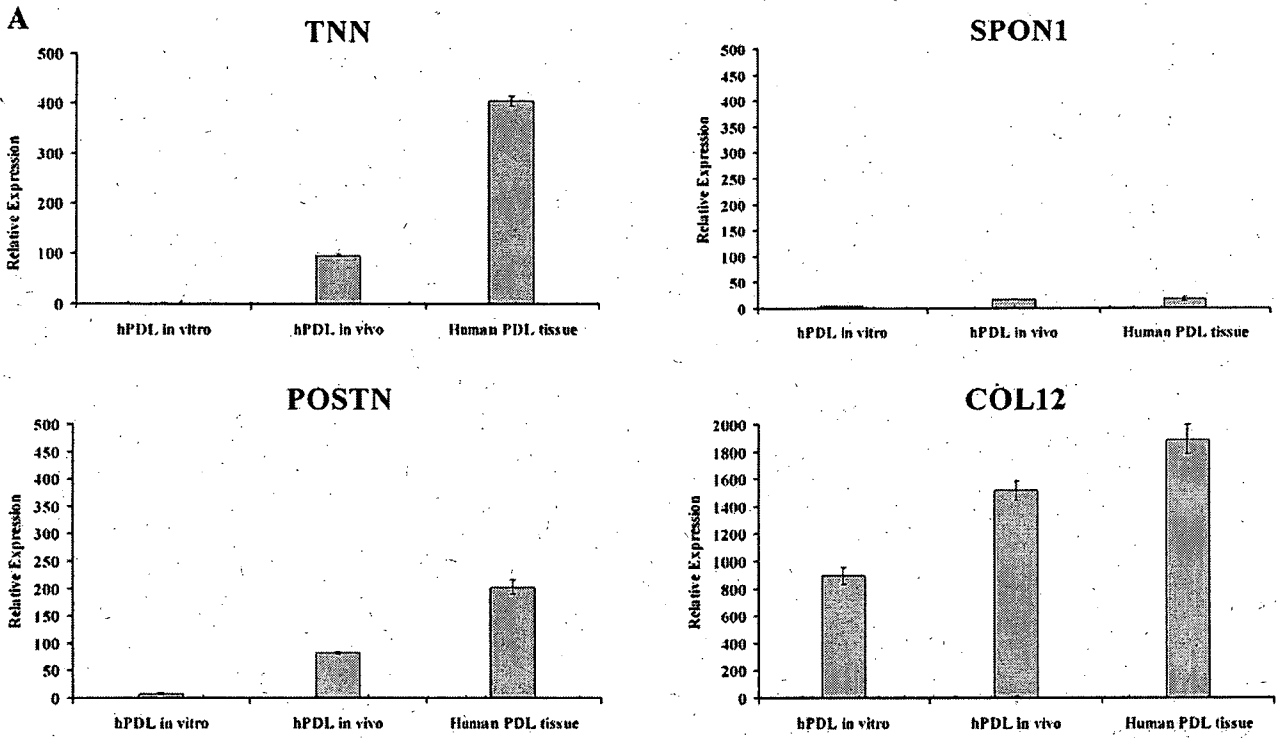
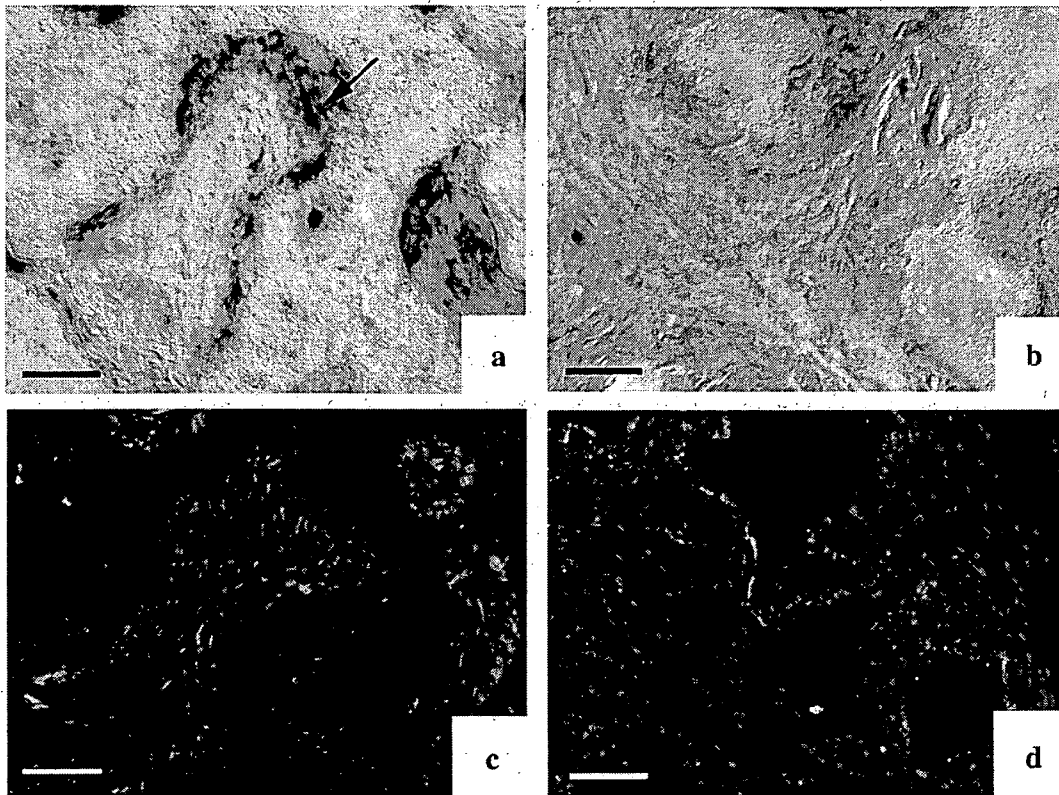


Fig. 3. Expression patterns of F-spondin and tenascin-N during early tooth germ development or tooth root formation. (A) During tooth germ development: F-spondin is initially expressed at the cap stage of DF in the tooth germ (b: arrow), and became intensely expressed in the bell stage and late stage of the DF (c and d: arrows). In contrast, expression of tenascin-N is not detected in the DF (e–h). However, tenascin-N expression is observed in dental mesenchymal cells at E13-bud stage (e: asterisk), and is also expressed in periosteum. E15-cap stage to P1-late bell stage (f–h: asterisks). Expression of periostin can be seen in dental mesenchyme in E13 tooth germ (i), and in DF during tooth germ development (j–l). bar: 100 μ m. (B) During tooth root formation: F-spondin is weakly expressed in root-forming stage of DF at P7 (a: arrow) and is not expressed in P35-adult molar PDL (b: arrow) as well as in adult incisor lingual side (c: arrow). Tenascin-N is not expressed in P7-root-forming stage of DF (d), however the expression was intensely up-regulated in P35-adult molar PDL (e: arrowhead). Specific expression of tenascin-N is also observed in adult incisor lingual side (f, arrowhead) although no expression is found in the labial side (f). Expression of periostin was observed in DF (g) and P35-adult molar PDL (h), but it is also detected in the preodontoblast layer (i: asterisk). bar: 100 μ m.



B



could not be detected in the DF cells at E15, E17, P1 and P7-DF of the developing tooth germ, (Fig. 3A, e–h, and Bd), but it was intensely up-regulated in the P35-PDL region where PDL cells enter terminal differentiation (Fig. 3Be). Mouse incisor showed asymmetrical distribution of PDL on the lingual side while no formation was found on the labial side. In the mouse incisor at P35, significant expression of tenascin-N was detected on the lingual side (Fig. 3Bf, arrowhead), whereas no expression was observed on the labial side (Fig. 3Bf). In contrast to tenascin-N, expression of F-spondin could not be detected in this region (Fig. 3Bc). In the control experiment, intense expression of periostin was observed in E13 dental mesenchyme and surrounding tissue (Fig. 3Ai). Consequently, periostin was expressed in DF at E15, E17 and P1-tooth germ (Fig. 3A, j–l). During tooth root-forming stage, periostin was expressed in DF, and strongly expressed in P35-PDL (Fig. 3B, g and h). However, strong expression was also detected in the preodontoblast layer of adult incisor (Fig. 3Bi).

3.5. *In vivo* differentiation of hPDL cells

Previous work has demonstrated that differentiation of cultured hPDL cells is induced upon implantation of these PDL cells into immunodeficient mice (Handa et al., 2002; Seo et al., 2004). We examined the expression of F-spondin and tenascin-N in cultured hPDL cells by real time PCR analysis to determine whether these genes are involved in differentiation of hPDL cells. Tenascin-N expression was not detected in cultured hPDL, but it was significantly induced in cells of the hPDL transplant 4 weeks after implantation (Fig. 4A). Contrary to tenascin-N, the expression of F-spondin in the cultured hPDL cells did not significantly differ from that in the hPDL transplant (Fig. 4A). In the control experiment, periostin expression slightly increased in the hPDL transplant (Fig. 4A). We also examined the mRNA expression level of type XII collagen as a control for PDL differentiation (Karimbux et al., 1992). Intense expression of type XII collagen was detected in cultured hPDL cells and it increased in the hPDL transplant (Fig. 4A). Expression patterns of these genes in the hPDL transplant were similar to that in human PDL tissue, indicating that hPDL cell differentiation was induced upon implantation into mouse (Fig. 4A). No expression of human tenascin-N, F-spondin, periostin and type XII collagen was detected in the transplants without human cells (data not shown). Expression of tenascin-N in the cells of the hPDL transplant was confirmed by *in situ* hybridization analysis. Results showed that significant tenascin-N expression was induced in the cells of the hPDL transplant (Fig. 4Ba). In addition, cells of the hPDL

transplant were positive for antibody against human specific vimentin (Fig. 4Bc). In the control site without implantation of hPDL cells, no positive signals were detected for tenascin-N and vimentin (Fig. 4B, b and d).

4. Discussion

4.1. Establishment of KK-Periome database and classification of ECM genes

Previous research has provided information on the expression of ECM genes during PDL formation (Karimbux et al., 1992; Takano-Yamamoto et al., 1994; Kruzynska-Frejtag et al., 2004). However, we still have limited knowledge regarding the transcriptional control of PDL development. Knowing the complexity of the process of PDL development, establishment of a gene expression profile database was considered useful, to identify the genes that play critical roles in the cascades of PDL development. Hence, we established the KK-Periome database that represents a collection of transcripts that are highly expressed in the human PDL. In the database, we found that unique ECM components such as F-spondin and tenascin-N are expressed at specific stages of DF and PDL during development. F-spondin was expressed in the early stage of DF, whereas tenascin-N expression was strongly induced upon PDL differentiation, suggesting that these genes/proteins represent markers for DF and PDL, respectively. Thus, the KK-Periome database has a potential to provide useful transcriptome information for investigating gene expression during PDL formation.

It was previously reported that PDL possessed a stem cell population that can differentiate into PDL, osteoblast and adipocyte (Seo et al., 2004). We also reported that a progenitor that can form PDL tissue was present in DF and PDL (Saito et al., 2005; Handa et al., 2002). From these findings, we hypothesized that both differentiated PDL-specific and immature PDL such as DF-specific markers could be identified from the KK-Periome database. To identify these markers, EST clusters in the KK-Periome database were analyzed by three different parameters such as expression frequency, functional classification and expression pattern: (1) EST clusters with expression frequency of more than three times were selected for inclusion in the KK-Periome database. (2) Since ECM is involved in tissue specificity, a list of ECM clusters was analyzed to determine whether the KK-Periome database reflects PDL phenotype. (3) Candidate genes that may play critical roles in the process of PDL development were selected

Fig. 4. Expression of F-spondin and tenascin-N in human periodontal ligament (hPDL) cells *in vitro* and *in vivo*. (A) Real time PCR analysis for tenascin-N (TNN), F-spondin (SPON), periostin (POSTN) and type XII collagen (COL12) and GAPDH *in vitro* and *in vivo*. Total RNA was isolated from hPDL cells (hPDL *in vitro*), hPDL cells of the transplant (hPDL *in vivo*) and human PDL tissue and subjected to real time PCR analysis. Level of TNN, SPON, POSTN and COL12A1 mRNA expression level were normalized against GAPDH level. Level of GAPDH mRNA expression was set at 100, and relative expression level was shown. Expression of TNN was intensely induced in hPDL transplants, while the expression level of SPON did not differ between cultured hPDL and hPDL transplants. Expression of both POSTN and COL12 was increased in hPDL transplants. Bar shows means \pm SD ($N=3$). (B) Expression of tenascin-N and vimentin in hPDL cells of the transplant. Sections of hPDL cells of the transplant (a, c) and transplants without cells (HAP transplants) (b, d) were analyzed by *in situ* hybridization with tenascin-N, or by immunohistochemistry with human specific vimentin antibody (c, d). Expression of tenascin-N is seen in the hPDL cells of the transplant (a). No expression of tenascin-N is seen in the HAP transplants used as negative control (b). hPDL cells of the transplant are positive for human specific vimentin monoclonal antibody (c) however, HAP transplant is negative for anti-vimentin antibody (d). Bar: 100 μ m.

by expression patterning with *in situ* hybridization analysis in mouse P1-DF and P35-PDL. As expected, the most abundantly expressed genes in the KK-Periome database were type I collagen and type III collagen, which are major fibrillar collagens in the PDL (Lukinmaa et al., 1993). Seven candidate genes with especially high expression in the PDL include SPARC, periostin, lumican, osteopontin, decorin, fibronectin and PLAP-1/Asporin (Takano-Yamamoto et al., 1994; Horiuchi et al., 1999; Yamada et al., 2001; Tenorio et al., 2003; Matheson et al., 2005). This expression profile was similar to the previous PDL-EST database (Yamada et al., 2001). Thus, the KK-Periome database reflects the PDL phenotype. In Table 3, 27 out of 39 EST clusters belonged to ECMs that are present in the PDL, providing additional evidence that the KK-Periome database represents the PDL phenotype. In the final step, we examined and compared the gene expression at the early stage of PDL formation (P1-DF) and the terminal differentiation stage (P35-PDL). F-spondin and tenascin-N were identified as candidate genes for early- and differentiation-stage markers, respectively. Periostin is a secreted adhesion protein that has homology with insect growth cone guidance protein fasciclin I (Horiuchi et al., 1999). During tooth germ development, periostin is expressed initially in the DF cells, and then restricted to postnatal PDL cells during the tooth root formation (Kruzynska-Frejtag et al., 2004). Periostin-deficient mice showed periodontal disease-like phenotype, suggesting a critical role of this protein in the maintenance of the PDL (Rios et al., 2005). Thus, periostin has been used as a marker for distinguishing PDL from adjacent connective tissues such as bone and gingiva in adult tissue (Saito et al., 2002; Yokoi et al., 2007). Although we were not investigating *periostin* splicing variant which is developmentally regulated by differential splicing (Kruzynska-Frejtag et al., 2004), *in situ* hybridization analysis and *in vivo* differentiation analysis revealed that expression of periostin could not distinguish adult PDL and DF cells. In contrast to periostin, F-spondin and tenascin-N were specifically expressed in DF and PDL respectively; furthermore *in vivo* differentiation analysis revealed that they are differentially expressed in PDL under *in vitro* and *in vivo* conditions. These findings strongly suggested that they might serve as PDL-lineage-specific markers.

4.2. F-spondin served as a marker for DF

The hypothesis that F-spondin is involved primarily in the initial process of PDL formation was further supported by our temporal and spatial expression analysis during tooth germ development. This is consistent with the notion that F-spondin may play a role in the early stage of PDL formation as demonstrated by the presence of high F-spondin mRNA level at E17 and P1-DF. Subsequently, F-spondin expression decreases dramatically at P35-PDL. In addition, *in vivo* differentiation assay revealed that F-spondin expression level did not change after implantation into SCID mice. Again, this is consistent with the idea that F-spondin may play a role in the early stage of PDL formation, especially those involved in PDL lineage. Although the precise function of F-spondin during tooth germ development

is not yet clear, F-spondin expression was observed in P1 dermal papilla cells. Many ectodermal tissues such as teeth and hair share similar epithelial–mesenchymal interactions during early development (Pispa and Thesleff, 2003). Our data indicated that expression of F-spondin is detected at the site of epithelial–mesenchymal interaction in the dermal papilla (Supplementary Fig. 1, a and c), suggesting that signaling molecules involved in ectodermal organogenesis regulated the expression of F-spondin.

4.3. Expression of tenascin-N was induced in differentiated PDL

In the present study, we observed strong tenascin-N expression in the P35-PDL. Interestingly, tenascin-N expression was detected in P1-perichondrocyte of rib (Supplementary Fig. 1b and f) that forms ligament tissue, suggesting that tenascin-N may be associated with ligament tissue formation. In contrast to F-spondin, tenascin-N expression was restricted to the terminally differentiated PDL. To determine whether tenascin-N expression was regulated by PDL differentiation, we carried out an *in vivo* differentiation assay in which hPDL cell differentiation could be promoted by implantation into immunodeficient mouse (Saito et al., 2005). Interestingly, tenascin-N expression was significantly induced in hPDL cells upon implantation while no expression was observed in the *in vitro* cultured cells. This data suggested that hPDL cells express tenascin-N as a result of differentiation. Spatial and temporal expression analysis during PDL development coincided with the *in vivo* differentiation study, suggesting that tenascin-N could serve as a marker for differentiated PDL. Expression of tenascin-N was observed in periosteum at P1 mandible, but it was more strongly expressed in P35-PDL where tenascin-N expression was barely detectable in periosteum. These findings support that tenascin-N could serve as an adult PDL marker.

In summary, we established the KK-Periome database that provides a resource to identify genes involved in PDL development. We found that specific ECMs such as F-spondin and tenascin-N could serve as markers for DF and PDL, respectively, although more work is necessary to verify the actual function of these proteins/genes. Nevertheless, spatial and temporal expression analysis indicated that F-spondin and tenascin-N are related to the PDL differentiation process during the development of PDL lineage. Thus, the KK-Periome database might contain invaluable information regarding the transcripts (transcriptome) that are closely associated with human PDL formation.

Acknowledgements

We thank Dr. Toshio Kawase for providing hPDL cells and Dr. Eiro Kubota for help in obtaining human PDL samples. We are also grateful to Drs. Naohito Nozaki, Sachiko Iseki, Takamasa Yokoi and Takanori Tsubakimoto for their helpful advice and discussions during the course of this work. This work was supported by a Grant-in Aid for High-Tech Research Center Project from the Ministry of Education, Culture, Sports, Science and Technology of Japan (MEXT) the AGU High-Tech Research Center Project, the 2003 Multidisciplinary Research Project from MEXT, and grants from MEXT.

Appendix A. Supplementary data

Supplementary data associated with this article can be found, in the online version, at doi:10.1016/j.gene.2007.09.009.

References

- D'Errico, J.A., MacNeil, R.L., Takata, T., Berry, J., Strayhorn, C., Somerman, M.J., 1997. Expression of bone associated markers by tooth root lining cells, in situ and in vitro. *Bone* 20, 117–126.
- D'Errico, J.A., et al., 1999. Immortalized cementoblasts and periodontal ligament cells in culture. *Bone* 25, 39–47.
- Hall, R.C., Embery, G., Lloyd, D., 1997. Immunochemical localization of the small leucine-rich proteoglycan in human predentine and dentine. *Arch. Oral Biol.* 42, 783–786.
- Handa, K., et al., 2002. Cementum matrix formation in vivo by cultured dental follicle cells. *Bone* 31, 606–611.
- Horiuchi, K., et al., 1999. Identification and characterization of a novel protein, periostin, with restricted expression to periosteum and periodontal ligament and increased expression by transforming growth factor beta. *J. Bone Miner. Res.* 14, 1239–1249.
- Hou, L.T., et al., 1999. Characterization of dental follicle cells in developing mouse molar. *Arch. Oral Biol.* 44, 759–770.
- Huang, X., Madan, A., 1999. CAP3: a DNA sequence assembly program. *Genome Res.* 9, 868–877.
- Huang, Y.H., Ohsaki, Y., Kurisu, K., 1991. Distribution of type I and type III collagen in the developing periodontal ligament of mice. *Matrix* 11, 25–35.
- Iseki, S., Wilkie, A.O., Heath, J.K., Ishimaru, T., Eto, K., Morriss-Kay, G.M., 1997. Fgfr2 and osteopontin domains in the developing skull vault are mutually exclusive and can be altered by locally applied FGF2. *Development* 124, 3375–3384.
- Karimbux, N.Y., Rosenblum, N.D., Nishimura, I., 1992. Site-specific expression of collagen I and XII mRNAs in the rat periodontal ligament at two developmental stages. *J. Dent. Res.* 71, 1355–1362.
- Kruzynska-Frejtag, A., et al., 2004. Periostin is expressed within the developing teeth at the sites of epithelial–mesenchymal interaction. *Dev. Dyn.* 229, 857–868.
- Lukinmaa, P.L., Vaahtokari, A., Vainio, S., Sandberg, M., Waltimo, J., Thesleff, I., 1993. Transient expression of type III collagen by odontoblasts: developmental changes in the distribution of pro-alpha 1(III) and pro-alpha 1(I) collagen mRNAs in dental tissues. *Matrix* 13, 503–515.
- Lukinmaa, P.L., Vaahtokari, A., Vainio, S., Thesleff, I., 1992. Expression of type I collagen pro-alpha 2 chain mRNA in adult human permanent teeth as revealed by in situ hybridization. *J. Dent. Res.* 71, 36–42.
- Lukinmaa, P.L., Waltimo, J., 1992. Immunohistochemical localization of types I, V, and VI collagen in human permanent teeth and periodontal ligament. *J. Dent. Res.* 71, 391–397.
- MacNeil, R.L., Berry, J.E., Strayhorn, C.L., Shigeyama, Y., Somerman, M.J., 1998. Expression of type I and XII collagen during development of the periodontal ligament in the mouse. *Arch. Oral Biol.* 43, 779–787.
- Matheson, S., Larjava, H., Hakkinen, L., 2005. Distinctive localization and function for fibromodulin and decorin to regulate collagen fibril organization in periodontal tissues. *J. Periodontol. Res.* 40, 312–324.
- Matsuura, T., Duarte, W.R., Cheng, H., Uzawa, K., Yamauchi, M., 2001. Differential expression of decorin and biglycan genes during mouse tooth development. *Matrix Biol.* 20, 367–373.
- McCulloch, C.A., 2006. Proteomics for the periodontium: current strategies and future promise. *Periodontology* 40, 173–183.
- Petersson, U., Hultenby, K., Wendel, M., 2003. Identification, distribution and expression of osteoadherin during tooth formation. *Eur. J. Oral Sci.* 111, 128–136.
- Pispa, J., Thesleff, I., 2003. Mechanisms of ectodermal organogenesis. *Dev. Biol.* 262, 195–205.
- Rios, H., et al., 2005. Periostin null mice exhibit dwarfism, incisor enamel defects, and an early-onset periodontal disease-like phenotype. *Mol. Cell Biol.* 25, 11131–11144.
- Sahlberg, C., Aukhil, I., Thesleff, I., 2001. Tenascin-C in developing mouse teeth: expression of splice variants and stimulation by TGFbeta and FGF. *Eur. J. Oral Sci.* 109, 114–124.
- Saito, M., et al., 2005. Immortalization of cementoblast progenitor cells with Bmi-1 and TERT. *J. Bone Miner. Res.* 20, 50–57.
- Saito, Y., et al., 2002. A cell line with characteristics of the periodontal ligament fibroblasts is negatively regulated for mineralization and Runx2/Cbfa1/Osf2 activity, part of which can be overcome by bone morphogenetic protein-2. *J. Cell Sci.* 115, 4191–4200.
- Salmivirta, K., Sorokin, L.M., Ekblom, P., 1997. Differential expression of laminin alpha chains during murine tooth development. *Dev. Dyn.* 210, 206–215.
- Sawada, T., et al., 2006. Immunohistochemical characterization of elastic system fibers in rat molar periodontal ligament. *J. Histochem. Cytochem.* 54, 1095–1103.
- Seo, B.M., et al., 2004. Investigation of multipotent postnatal stem cells from human periodontal ligament. *Lancet* 364, 149–155.
- Shibata, S., Yoneda, S., Yanagishita, M., Yamashita, Y., 2002. Developmental changes and regional differences in histochemical localization of hyaluronan and versican in postnatal molar dental pulp. *Int. Endod. J.* 35, 159–165.
- Shibata, Y., Fujita, S., Takahashi, H., Yamaguchi, A., Koji, T., 2000. Assessment of decalcifying protocols for detection of specific RNA by non-radioactive in situ hybridization in calcified tissues. *Histochem. Cell Biol.* 113, 153–159.
- Sloan, P., Carter, D.H., Kielty, C.M., Shuttleworth, C.A., 1993. An immunohistochemical study examining the role of collagen type VI in the rodent periodontal ligament. *Histochem. J.* 25, 523–530.
- Takano-Yamamoto, T., Takemura, T., Kitamura, Y., Nomura, S., 1994. Site-specific expression of mRNAs for osteonectin, osteocalcin, and osteopontin revealed by in situ hybridization in rat periodontal ligament during physiological tooth movement. *J. Histochem. Cytochem.* 42, 885–896.
- Ten Cate, A.R. (Ed.), 1994. *Oral Histology, Development, Structure, and Function*. Mosby, St. Louis.
- Tenorio, D.M., Santos, M.F., Zorn, T.M., 2003. Distribution of biglycan and decorin in rat dental tissue. *Braz. J. Med. Biol. Res.* 36, 1061–1065.
- Tsubota, M., Sasano, Y., Takahashi, I., Kagayama, M., Shimauchi, H., 2002. Expression of MMP-8 and MMP-13 mRNAs in rat periodontium during tooth eruption. *J. Dent. Res.* 81, 673–678.
- Venter, J.C., Levy, S., Stockwell, T., Remington, K., Halpern, A., 2003. Massive parallelism, randomness and genomic advances. *Nat. Genet.* 33, 219–227.
- Wilkinson, D.G., 1995. RNA detection using non-radioactive in situ hybridization. *Curr. Opin. Biotechnol.* 6, 20–23.
- Worapamorn, W., Li, H., Pujic, Z., Xiao, Y., Young, W.G., Bartold, P.M., 2000. Expression and distribution of cell-surface proteoglycans in the normal Lewis rat molar periodontium. *J. Periodontol. Res.* 35, 214–224.
- Yamada, S., et al., 2001. Expression profile of active genes in human periodontal ligament and isolation of PLAP-1, a novel SLRP family gene. *Gene* 275, 279–286.
- Yokoi, T., et al., 2007. Establishment of immortalized dental follicle cells for generating periodontal ligament in vivo. *Cell Tissue Res.* 327, 301–311.

ORIGINAL ARTICLE

Eleni Hji Antoniou · Mustafa Anayasa · Paschalis Nicolaou · Ioannis Bantounas · Masahiro Saito · Sachiko Iseki · James B. Uney · Leonidas A. Phylactou

Twist induces reversal of myotube formation

Received December 20, 2006; accepted in revised form May 3, 2007

Abstract Mammals possess reduced ability to regenerate lost tissue, compared with other vertebrates, which can regenerate through differentiation of precursor cells or de-differentiation. Mammalian multinucleated myotube formation is a differentiation process, which arises from the fusion of mononucleated myoblasts and is thought to be an irreversible process toward muscle formation. By overexpressing the Twist gene in terminally differentiated myotubes, we managed to induce reversal of cell differentiation. More specifically, following expression of the Twist gene, myotubes underwent morphological changes that caused them to cleave. This was accompanied by a reduction in the expression of certain myogenic markers. Interestingly,

Twist overexpression also caused a reduction in the muscle transcription factor MyoD. Further experiments showed an increase in the cell cycle entry molecule, cyclin D1 and initiation of DNA synthesis, due to Twist overexpression. The exploitation of Twist-mediated reversal of differentiation and the study of its specific mechanism would be important in order to study mammalian cellular de-differentiation and determine its potential in muscle regeneration.

Key words twist · myotubes · reversal of differentiation

Eleni Hji Antoniou · Mustafa Anayasa · Paschalis Nicolaou · Leonidas A. Phylactou (✉)
The Cyprus Institute of Neurology & Genetics
P.O. Box 23462, 1683 Nicosia, Cyprus
Tel: +357 22 358600
Fax: +357 22 358237
E-mail: laphylac@cing.ac.cy

Ioannis Bantounas · James B. Uney
The Henry Wellcome Laboratories for Integrative Neuroscience and Endocrinology, Dorothy Hodgkin Building
University of Bristol, Whitson Street
Bristol BS1 3NY, U.K.

Masahiro Saito
Department of Molecular and Cellular Biochemistry
Osaka University
Graduate School of Dentistry
Yamadaoka 1-8
Suita City
Osaka 565-0871
Japan

Sachiko Iseki
Section of Molecular Craniofacial Embryology
Graduate School, Tokyo Medical and Dental University
1-5-45 Yushima, Bunkyo-ku, Tokyo 113-8549, Japan

Introduction

While vertebrates like salamanders, zebrafish, and *Xenopus laevis* have developed advanced regenerative abilities, mainly through differentiation of precursor cells or de-differentiation, mammals have a limited capacity to regenerate (Odelberg et al., 2000). Differentiation of mammalian cells is thought to be a terminal and irreversible process. The *in vitro* differentiation of myocytes into myotubes is a well-characterized example of terminal differentiation (Andres and Walsh, 1996; Sers et al., 1997). Myoblasts are skeletal muscle cells that are capable of cell proliferation in the presence of growth factors. They could also enter terminal differentiation when grown to confluency and deprived of growth factors. Differentiated cells fuse to form multinucleated myotubes in an irreversible procedure. Currently, there is very little evidence for mammalian cellular reversal of differentiation. Researchers, however, have been trying to induce de-differentiation in mammalian cells, mostly *in vitro*. Because it forms a good model, most of the previous experiments to study myotube de-differentiation were carried out in the mouse C2C12 cell line. When newt and mouse myoblasts were allowed to fuse together

in vitro both cell nuclei could re-enter the cell cycle by responding to thrombin and serum (Kumar et al., 2004). Another study showed that newt extracts could induce mouse myotubes to reinitiate the cell cycle (McGann et al., 2001). Overexpression of the *Msx-1* gene in myotubes caused their cleavage into proliferating mononucleated cells, which could trans-differentiate into other cell types (Odelberg et al., 2000). Myoseverin, a trisubstituted purine, also caused mammalian myotube de-differentiation (Rosania et al., 2000). Recently, introduction of the *CSX/Nkx2.5* transcription factor caused a change of morphology of myotubes and cleavage into smaller parts but without any apparent cell cycle activity (Riazi et al., 2005). The exact mechanism of induced de-differentiation and its *in vivo* potential however remains yet to be seen. Mammalian de-differentiation is a new research field that will provide additional basic knowledge about mechanisms of mammalian regeneration. The identification of molecules, which can induce or are involved in de-differentiation, is of vital importance (Echeverri and Tanaka, 2002).

Twist is a nuclear basic helix-loop-helix (bHLH) transcription factor, crucial for mesoderm formation in *Drosophila* (Thisse et al., 1988). The HLH motif was first identified in the murine DNA-binding proteins E12 and E47 (Murre et al., 1989). In mammals, Twist is mostly expressed in cranial neural crest derivatives and in mesenchymal structures (Bate et al., 1991; Hebrok et al., 1994; Fuchtbauer, 1995; Gitelman, 1997) and its expression has been implicated in the inhibition of differentiation of several mesodermal cell lineages, including muscle (Hebrok et al., 1994; Spicer et al., 1996), cartilage (Poliard et al., 1995), and bone (Murray et al., 1992; Lee et al., 1999). Mutations in the *TWIST* gene are responsible for the Saethre-Chotzen syndrome, an autosomal dominant craniosynostosis characterized by abnormal fusion of the cranial sutures (el Ghouzzi et al., 1997; Howard et al., 1997). bHLH proteins bind as dimers to a consensus sequence E-box through their basic domain (Ephrussi et al., 1985). Several experiments indicate that the Twist family members bind preferentially to the E-box of MyoD/E heterodimers, as homodimers (Lee et al., 1999; Kophengnavong et al., 2000) or heterodimers (Spicer et al., 1996) with the E protein family. Moreover, the basic domain of murine Twist has been reported to physically interact with the basic domain of MyoD (Hamamori et al., 1997). The association between these basic regions is implicated as one mechanism by which Twist can regulate myogenesis in vertebrates.

Apart from its role in control of cell differentiation, Twist has been found to be involved in cancer. Overexpression of Twist has been reported in several types of cancer, including invasive lobular breast carcinomas (Yang et al., 2004), T-cell lymphomas (van Doorn et al., 2004), and rhabdomyosarcomas (Maestro et al., 1999). Finally, a role for Twist in programmed cell death has

been revealed. It has been reported that Twist antagonizes p53-dependent apoptosis and growth arrest (Maestro et al., 1999) and that Twist overexpression is associated with acquired drug resistance in human cancer cells (Wang et al., 2004). Moreover, it has been shown that Twist is involved in insulin-like growth factor-1 (IGF-1) receptor-mediated protection and modulation of tumor necrosis factor- α (TNF- α)-dependent apoptosis (Dupont et al., 2001) and that by using artificial catalytic DNA molecules (DNazymes), down-regulation of Twist gene expression increases cellular apoptosis (Hjiantoniou et al., 2003).

In this paper, we show yet another novel and important aspect of the Twist function. We show that overexpression of the Twist gene in differentiated mouse muscle cells induces reversal of muscle differentiation.

Methods

Cloning and generation of recombinant adenovirus constructs

Mouse Twist cDNA and a control sequence (an inactive hammerhead ribozyme against Twist RNA that has been shown not to cause any reduction in Twist RNA, protein levels—data not shown) were cloned in vectors for adenoviral production. Recombinant E1-deleted adenoviral constructs were produced as described before (Glover et al., 2002).

Tissue culture

C2C12 mouse myoblasts were grown to confluency in growth media (GM), Dulbecco modified eagle's medium (DMEM) with 10% fetal bovine serum (FBS) and 2 mM glutamine (Invitrogen, Carlsbad, CA). They were then switched to differentiation media (DM), DMEM, 4% Horse Serum, and 2 mM glutamine for up to 4 days for myotube formation. For adenoviral transfections, 50 MOI were incubated with myoblasts for inhibition of differentiation or with myotubes for de-differentiation studies for 48 hr in DM. Transfected and untransfected myotubes were incubated further in GM or split by gentle trypsinization (0.25% trypsin/1 mM ethylene diamine tetraacetic acid [EDTA]) and transferred to 60 mm plates coated in 0.75% gelatin (Sigma, St. Louis, MO) in DM at a density of 1–2 myotubes/mm². In the case of split cells, the following day, carried-over myoblasts were killed by pipette tip ablation and the media was replaced by fresh DM for another 24 hr. Myotubes were then incubated with GM, marked, and digital images taken under an inverted microscope (Nikon TE2000E, Nikon, Japan) or processed for other studies. Two hundred and fifty to 350 myotubes were evaluated for each experiment.

RNA analysis

Total RNA was extracted from transfected or untransfected myotubes (Perfect RNA Eukaryotic Mini kit, Eppendorf, Germany) and subjected to reverse transcription. For detection of the Twist RNA in myotubes by polymerase chain reaction (PCR), Twist (fwd 5'-CCCAAGCTTGTCTACGAGGAGCTGCAGA-3', rev 5'-CGCGGATCCCTCCAGACGGAGAAGGCGTA-3') primers were used under quantitative conditions. For detection of molecular changes by RT/PCR, following transfections, MyoD (fwd 5'-CCC CGCTCCA ACTGCTCTGAT-3, rev 5'-CCTACGGTGGT GCGCCCTCTGC-3'), *cdk4* (fwd 5'-CAGCACTCCTACCTG

CACAA-3', rev 5'-AGGAGAGGTGGGGACTTGTT-3'), *cycD1* (fwd 5'-GGCACCTGGATTGTTCTGTT-3', rev 5'-CAGCTTGCTAGGGAACCTGG-3'), *MEF2* (fwd 5'-GAATGCCCAAAGGATAAGCA-3', rev 5'-TGTCTAGATGGTGCTGCTG-3'), and glyceraldehyde-3-phosphate dehydrogenase (*GAPDH*) primers (fwd 5'-TCATCATCTCCGCCCTCC-3' and rev 5'-GAGGGCCATCCACAGTCTT-3') primers were used after determining quantitative conditions (27, 27, 28, 26, and 25 cycles, respectively). For quantitative studies, experiments were repeated at least six times and gel bands were measured using Scion Image software.

Western blotting

Twenty to 30 μ g of protein extracts were incubated with the Twist antibody (1:200) or caspase-3 antibody (1:7,000, Santa Cruz, Santa Cruz, CA) followed by incubation with a goat anti-mouse immunoglobulin G (IgG) or donkey anti-rabbit secondary antibodies, respectively, conjugated to horseradish peroxidase (Santa Cruz).

Immunofluorescent studies

Myotubes were incubated with various antibodies after 0–3 days of GM induction. Briefly, cells were fixed in 4% paraformaldehyde and blocked in 1% Triton X-100 dissolved in 1% bovine serum albumin (BSA) in phosphate-buffered saline (PBS). Myotubes were then exposed to myosin heavy chain (MHC) (MY32 Sigma 1:400), myogenin (1:200, Santa-Cruz), MyoD (1:100 Pharmingen, San Diego, CA), and Twist (1:400) antibodies for 1 hr at 37°C and then incubated with the following secondary antibodies: a goat anti-mouse Texas Red, a goat anti-rabbit Texas Red, and a goat anti-mouse fluorescein isothiocyanate (FITC) antibody (Jackson ImmunoResearch, West Grove, PA) for 30 min at room temperature and nuclei were stained with 4,6-diamidino-2-phenylindole (DAPI) (Vysis, Downers Grove, IL). Cells were visualized under a Nikon Eclipse 2000 inverted microscope, images acquired by DXM1200F digital camera (Nikon), and analyzed by Adobe Photoshop software.

Cell cycle studies

Myotubes incubated in GM up to 2 days were then supplemented with 50 μ M bromodeoxyuridine (BrdU) (Sigma) for a further 24 hr, followed by fixation at room temperature. Cells were then permeabilized as described above. The cells were then denatured with 2N HCl for 30 min at 37°C and then blocked in 1% BSA in PBS for 10 min. Myotubes were then exposed to anti-BrdU mouse antibody (Sigma) for 1 hr at 37°C and then after washing with PBS were exposed to a goat anti-mouse secondary antibody for 30 min at room temperature.

DNA analysis for apoptosis

DNA extractions were carried out using the DNeasy Tissue Kit (Qiagen, Germany) and then concentrated in the SpeedVac Concentrator (Savant SVC100H, Savant, Rochester, NY). Equal amounts of DNA samples were loaded on 1.8% agarose gel. The DNA was visualized by ultraviolet (UV) illumination.

Results

An E1-deleted adenovirus, carrying the mouse Twist cDNA (AdT), was constructed. Twist is known to in-

hibit myogenesis (Hebrok et al., 1994); hence, in order to determine whether AdT produced functional Twist, C2C12 myoblasts were transduced with the recombinant virus. A control adenovirus (AdC), expressing an inactive hammerhead ribozyme sequence, was also used.

Following transfections, myoblasts were induced to become multinucleated myotubes with differentiation medium. There was a marked inhibition of myogenesis in cells transfected with the AdT, compared with AdC-transfected and untransfected myoblasts, which fused normally into myotubes (Fig. 1A).

Having shown that the AdT viral vector can transduce mouse myoblasts and inhibit the formation of multinucleated myotubes, its efficiency to transfect already formed myotubes was checked at the RNA and protein levels (Figs. 1B, 1C). Overproduction of Twist mRNA was detected in C2C12 myotubes transfected with the AdT viral vector whereas control-transduced cells (AdC) showed no increase in Twist mRNA levels compared with the endogenous levels (Fig. 1B). Moreover, Western blot analysis detected overexpression of Twist protein (Fig. 1C), compared with untransfected cells or cells transfected with the control adenovirus (AdC) with a Twist antibody, which is known to detect only transgene Twist product (unpublished data).

Three days after the transfection with the Twist-expressing adenoviral vector, there were fewer myotubes present compared with the untransfected or with those transfected with the AdC (Fig. 2A). Overexpression of the Twist gene in terminally differentiated myotubes seemed to have caused their elimination from the culture.

In order to clarify and characterize in more detail the effect of the overexpression of the Twist gene on multinucleated myotubes, a method was developed similar to the one reported before (Odelberg et al., 2000) to isolate individual myotubes. By using a specific protocol in which differentiated cells were detached from the cultured plate and separated from the myoblasts, individual myotubes were observed under a microscope over a period of time. A significant proportion of myotubes transfected with the AdT viral vector (28%) underwent cleavage (Figs. 2B, 2C). At the beginning myotube structure was distorted, followed by the cleavage into smaller cellular parts. This occurred mainly in two ways: cleavage was around the areas where the nuclei reside (Fig. 2B) and cleavage took place in the middle of the myotube, following separation of the nuclei into the two cellular halves (Fig. 2C). No cleavage was seen in any of the untransfected myotubes (Fig. 2D) or in myotubes transfected with the control virus, AdC (Fig. 2E), indicating the specificity of cleavage by Twist. Since fusion of myoblasts is the procedure that forms multinucleated myotubes, these results indicate that overexpression of the Twist gene might be inducing reversal of cell differentiation.

The results described above indicate that the overexpression of the Twist gene induces myotubes to undergo

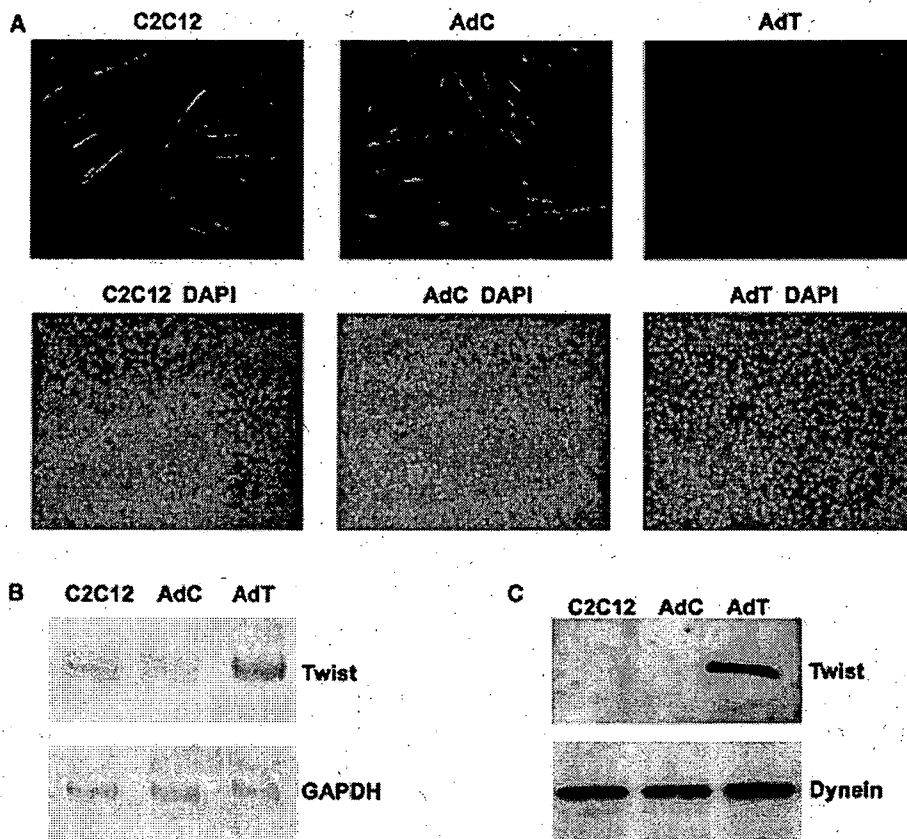


Fig. 1 Twist inhibits myotube formation and is overexpressed in myotubes. (A) C2C12 myoblasts were transfected with a Twist-expressing adenovirus (AdT) or a control adenovirus (AdC) and were induced to differentiate for 3 days as shown by MHC immunostaining and nuclear staining by DAPI. Whereas both AdC transfected and untransfected C2C12 cells readily formed myotubes,

overexpression of Twist cDNA did not. Transfection of AdT in mouse myotubes caused an overexpression of the Twist cDNA (AdT) as detected by RT/PCR (B) and Western blotting (C), compared with control-transfected cells (AdC) and untransfected cells. DAPI, 4,6-diamidino-2-phenylindole; PCR, polymerase chain reaction; MHC, myosin heavy chain.

structural changes leading to their cleavage. Myotube formation is always accompanied by an increase of several myogenic markers and the termination of cell cycle (Tajbakhsh, 2005). Since the overexpression of the mouse Twist cDNA showed signs of cell differentiation reversal, as a next step the levels of an early and a late myogenic marker were investigated.

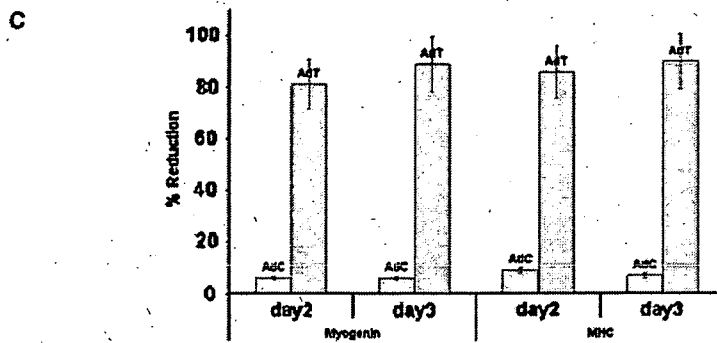
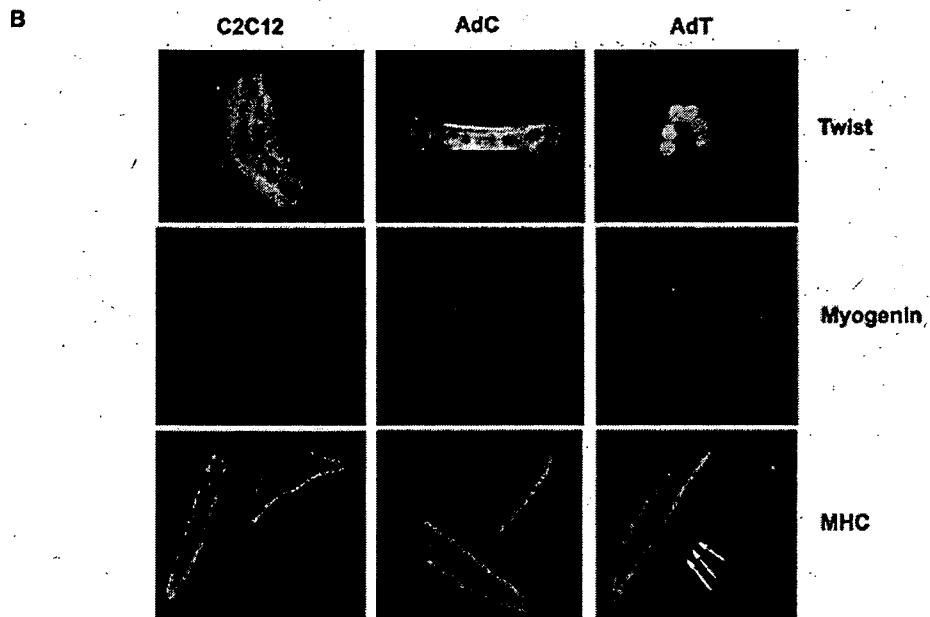
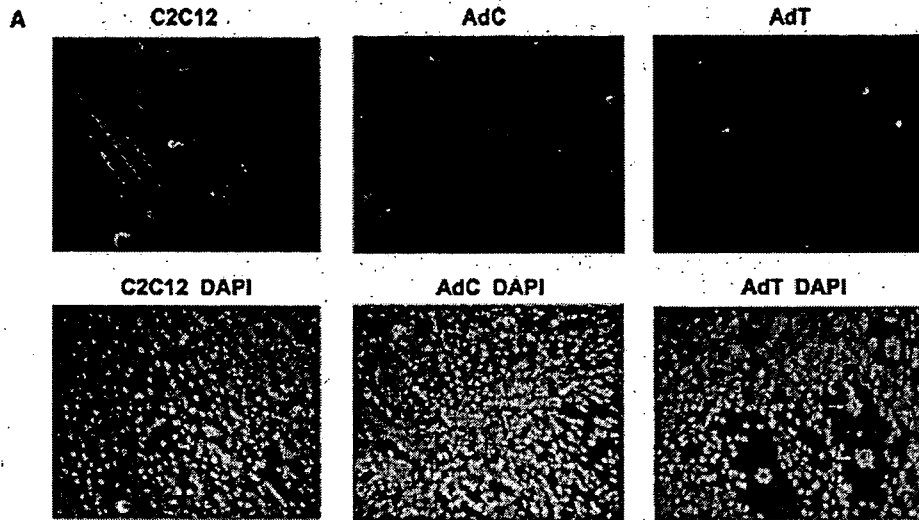
Immunodetection of the MHC, a late marker of myogenesis, revealed a heavy reduction in the expression of the MHC gene. The decrease was very pronounced 3 days after the transfection of the viral vector AdT (Fig. 3A). Normal staining was observed in untransfected cells or in cells transfected with the control viral vector AdC. Moreover, nuclear staining of the cells transfected with the AdT viral vector shows areas where the nuclei are clustered in the two ends of the myotube, presumably before cleavage, which was also demonstrated in Figure 2C. In order to perform a more detailed analysis, immunodetection of MHC and also of myogenin (an early marker of myogenesis) was performed on individual myotubes. Following transfection with the Twist-expressing adenovirus

(AdT), immunodetection revealed a reduction in the expression of myogenin and MHC, whereas untransfected cells or cell transfected with the control viral vector AdC maintained their normal myogenin and MHC levels (Fig. 3B). In an attempt to quantitate the effect of Twist on both these proteins whose levels are high during the process of differentiation, myotubes that did not stain for myogenin or MHC were counted 2 and 3 days after the introduction of GM to the cells (Fig. 3C). Both levels of myogenin and MHC showed a dramatic reduction in the myotubes transfected with the Twist cDNA with an increasing trend over time. Because both these molecules are involved during muscle cell differentiation and the induction of their gene expression accompanies muscle formation, these results imply that among other things, Twist overexpression in multinucleated myotubes causes reduction of proteins that are involved in myogenesis.

Having seen a reduction in the markers of muscle formation and cleavage of differentiated myotubes, resembling reversal of differentiation, experiments were continued in order to investigate whether cell cycle re-

activation takes place. This was carried out by detecting possible changes in molecules that play a key role in this process. One of the myogenic regulatory factors, MyoD, a transcription factor, up-regulated during the

exit of muscle cells from the cell cycle and induced during myogenesis, was chosen as a first target. MyoD RNA levels were substantially reduced in cells transfected with the overexpressing Twist adenoviral vector



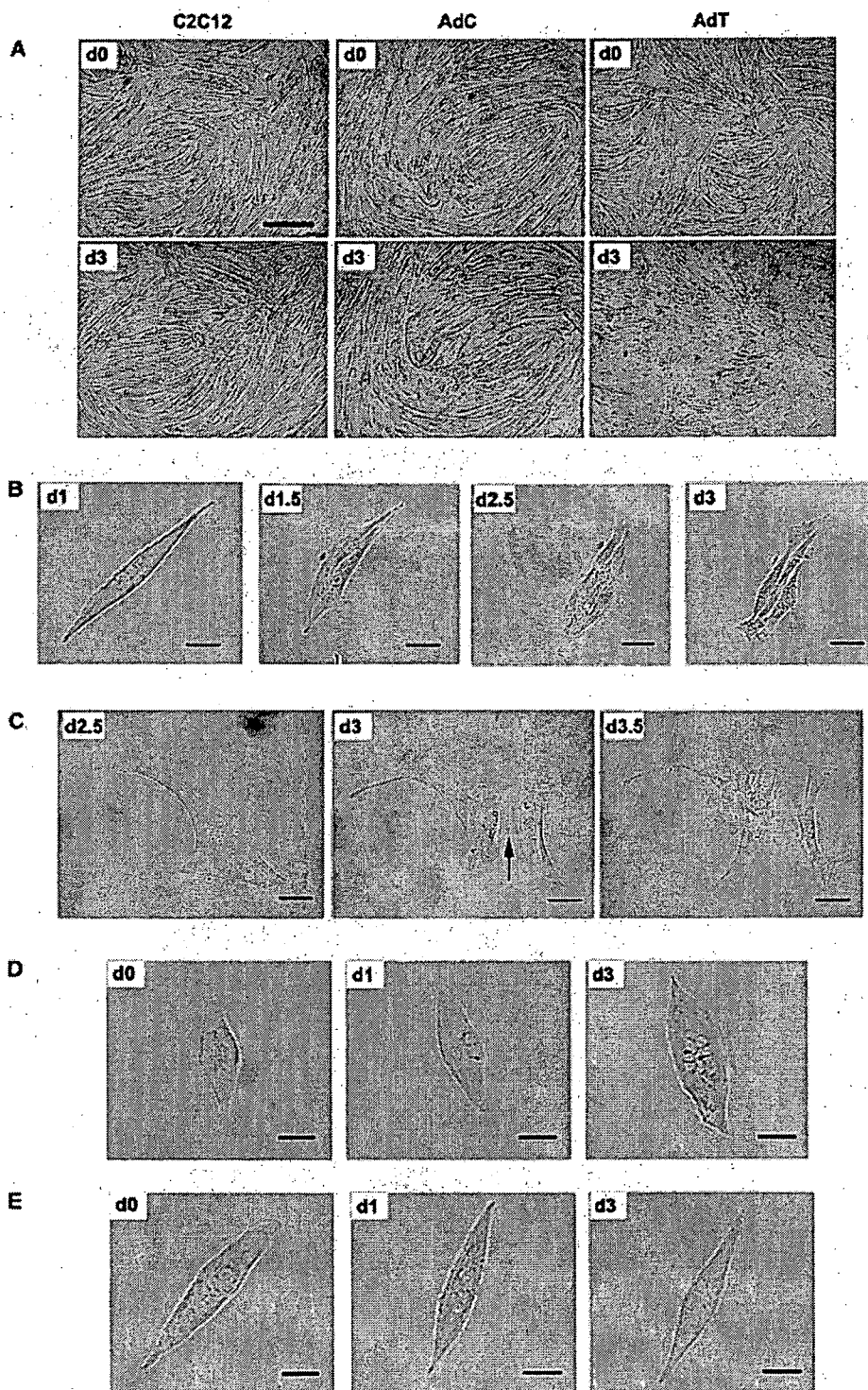


Fig. 2 Twist overexpression caused morphological changes in myotubes. (A) Following muscle cell differentiation for 4 days (d0), cells were transfected with the Twist-expressing virus (AdT), the control virus (AdC) for 2 days and then incubated for 24 hr (d3) in growth medium. AdT transfection caused a reduction of myotubes. (B) Twist overexpression causes cleavage of individual multinucleated myotubes in mainly two ways. Following AdT transfection and

incubation in GM, the myotube (d1) was torn and cleaved around the nuclei (d1.5–d3). (C) In the second way, myotubes were cleaved in the middle (indicated by an arrow), following the separation of the nuclei in the two cellular halves. No cleavage was seen in untransfected (C2C12) (D) and control-transfected myotubes (AdC) (E). Scale bars represent 0.05 cm. GM, growth medium.

(Fig. 4A). It was found that MyoD levels in cells transfected with the Twist gene were more than 50% lower than the control cells (Fig. 4D). Moreover, immunocytochemistry experiments were performed to determine MyoD protein levels in Twist-transfected cells. Similar to the RNA levels, MyoD protein levels were reduced (Fig. 4B). Proper MyoD staining was observed in cells transduced with the control AdC viral vector and in untransfected cells. These results show that overexpression of the Twist gene has a negative effect on the expression of the MyoD, which is a known important factor for myogenesis to happen. Because MyoD reduction levels were found reduced following the overexpression of the Twist gene, various other molecules involved in cell cycle and differentiation were checked. Cyclins and cyclin-dependent kinases (cdks) form complexes and control several key points of the cell cycle. The RNA levels of Cyclin D1, which is usually involved in the first steps of cell cycle activation, were found elevated only in cells transfected with the AdT (Figs. 4C,4D). No significant changes were seen in its partner cdk4 and MEF2, the molecule that conjugates with MyoD during myogenesis (Fig. 4C). Therefore, these results have provided evidence about the reactivation of the cell cycle following the expression of the Twist gene in the terminal differentiated mouse myotubes. This evidence comes from the gene expression changes detected in molecules involved in myogenesis and in the cell cycle.

In order to exclude the possibility that Twist induces apoptosis or necrosis in transfected myotubes, two assays were performed to determine whether this happens. A DNA (ethidium bromide) assay (early apoptosis step) and a Western blot to detect caspase levels, known to be increased during apoptosis (late apoptosis step), were carried out (Figs. 4E,4F). Ethidium bromide assay showed no DNA fragmentation and the smear observed, which denotes some necrosis in the myotubes, was similar between the Twist-transduced cells (AdT) and the control-transduced cells (AdC) and was less in the untransfected C2C12 cells. This is probably necrosis due to the transduction of viral vectors, which is added to the known minor necrosis observed in differentiated muscle cells (Shiokawa et al., 2002). Moreover, Western blot analysis showed no caspase-induced apoptosis, in cells transfected with the Twist viral vector (AdT),

compared with untransfected C2C12 cells or cells transfected with the control viral vector (AdC), indicating that Twist does not cause early or late apoptosis to the transduced myotubes. This agrees with other reports which showed that Twist not only causes apoptosis but can also act as an anti-apoptotic molecule (Maestro et al., 1999; Hjianioniou et al., 2003; Demontis et al., 2006).

Since DNA synthesis is the first step in cell cycle activation, further experiments were performed in order to observe such events in myotubes transfected with the AdT viral vector. For this purpose, Twist-transfected cells were incubated with BrdU. Immunostaining revealed that there was an initiation of DNA synthesis, compared with untransfected or AdC-transfected cells, which remained outside the cell cycle (Fig. 5A). In order to investigate in more detail the initiation of DNA synthesis coupled to the reduction of muscle cell markers MyoD, myogenin, and MHC, triple immunocytochemistry experiments were carried out (Figs. 5B-5D). These experiments reconfirmed that Twist expression causes reduction in the levels of all three molecules (MyoD, myogenin, and MHC) accompanied by the active DNA replication in those cells (Fig. 5B). However, it was interesting to observe that at an earlier stage the Twist expression could only induce a reduction in the levels of myogenic molecules but not in DNA synthesis (Fig. 5C). These results imply that although cells enter the cycle, this happens at a relatively later stage. Positive staining for the three myogenic markers and absence of BrdU staining was observed in untransfected cells (Fig. 5D) and cells transfected with the control adenoviral vector, AdC (data not shown). Finally, triple immunocytochemistry experiments revealed cleaved cells with positive BrdU staining following transfection with the AdT Twist adenoviral vector (Fig. 5E). Moreover, these cells were negative for MyoD and MHC molecules.

Discussion

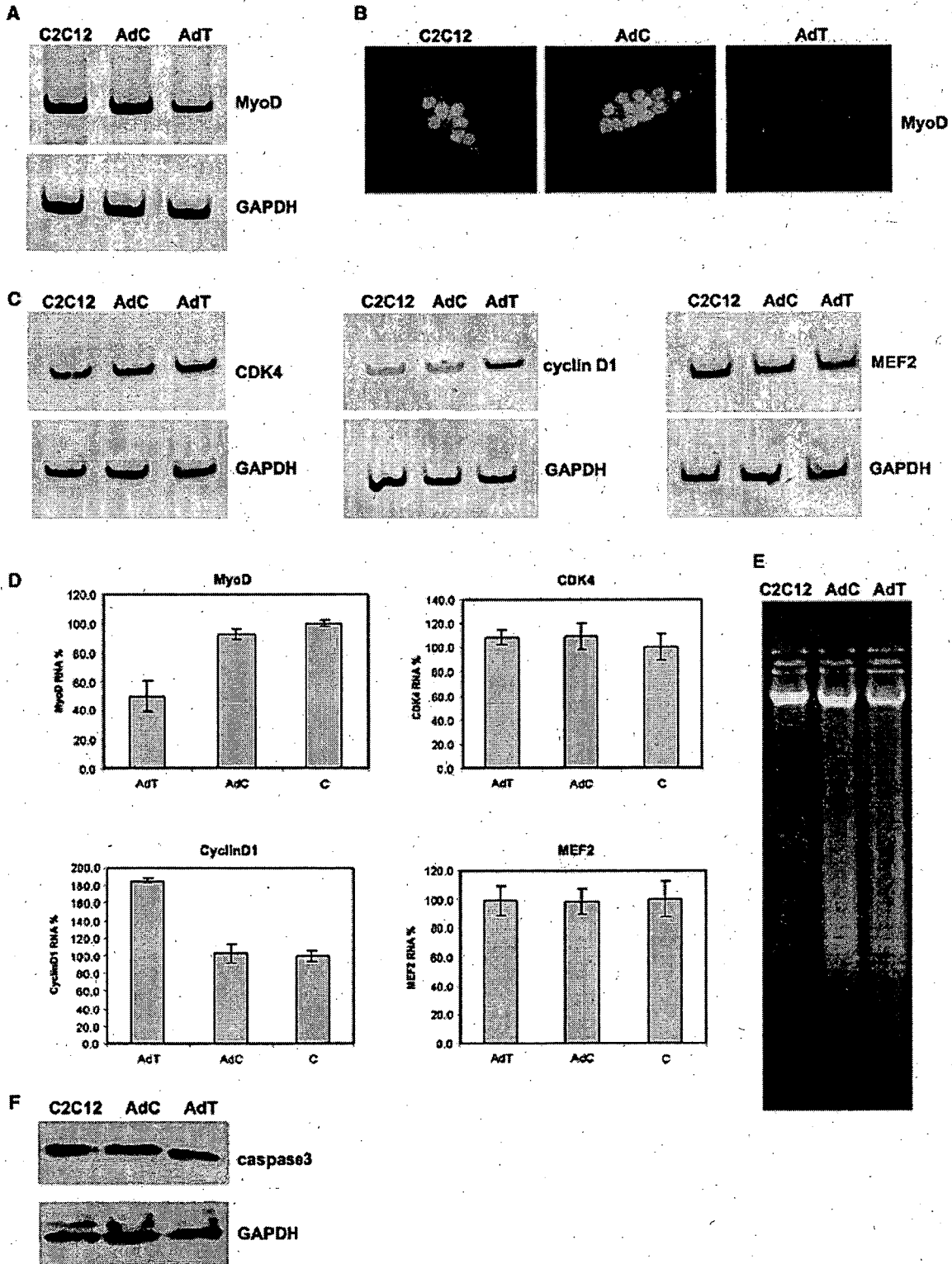
These results show that the overexpression of the Twist gene in terminally differentiated muscle cells (myotubes) can re-activate those cells and induce the reversal of

Fig. 3 Reversal of muscle differentiation markers. (A) Following myotube differentiation for 4 days, cells were transfected with the Twist-expressing virus (AdT), the control virus (AdC) for 2 days and then incubated for 24 hr (d3) in growth medium. Myotubes were fixed and stained with an MHC antibody and marked with DAPI. White arrows indicate the clustering of the nuclei in the two ends of the myotube, in AdT-transfected cells. (B) Myotubes expressing the Twist cDNA via the AdT viral vector caused a reduction in myogenin and MHC muscle differentiation markers, as detected by immunohistochemistry, compared with untransfected

(C2C12) and control-transfected individual cells (AdC). Negative staining for myogenin is demonstrated with the absence of nuclear staining, whereas background MHC levels demonstrate negative staining for MHC. (Note that the MHC immunofluorescence images had to be overexposed in order to see a negatively stained myotube, as shown by the arrows.) (C) In order to get a quantitation for myogenin and MHC on the negatively stained cells by immunofluorescence, cells were counted and then calculated as a proportion of the untransfected cells. MHC, myosin heavy chain; DAPI, 4,6-diamidino-2-phenylindole.

their differentiation. These myotubes change morphology and eventually cleave into smaller cell products. This cellular cleavage was accompanied by a reduction in early and late markers of muscle differentiation fol-

lowed by re-activation of the DNA machinery as detected by BrdU incorporation. Regarding the mechanism of the Twist-induced reversal of muscle cell differentiation, the myogenic transcription factor,



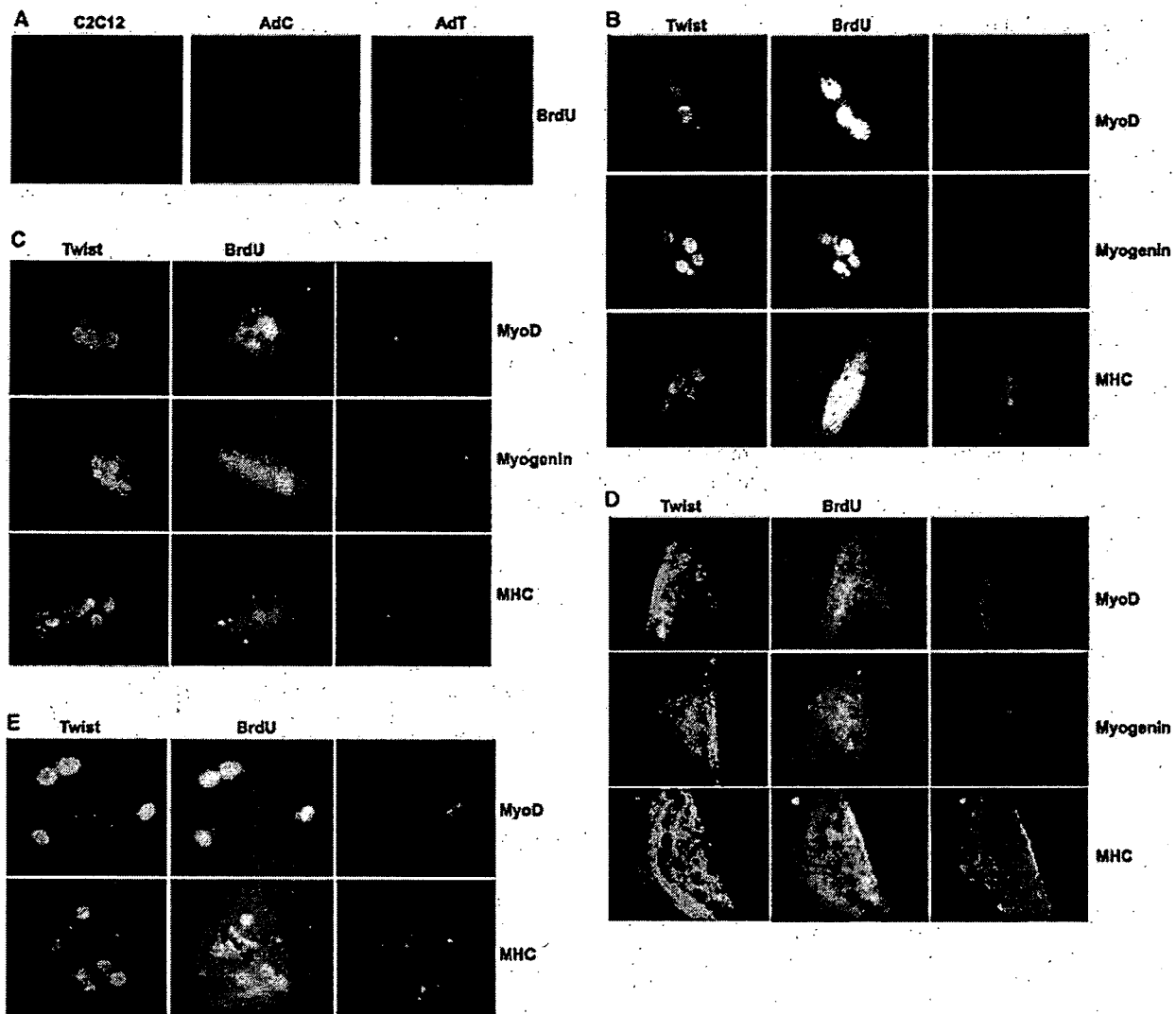


Fig. 5 Reduction of myogenic markers MyoD, myogenin, and MHC followed by re-entry to the cell cycle and accompanied by myotube cleavage. (A) Overexpression of the Twist cDNA (AdT) caused an increase in BrdU-positive cells as shown with the intense nuclear coloring compared with untransfected (C2C12) and control-transfected cells (AdC). (B) Reduction of myogenic markers MyoD, myogenin, and MHC occurred after transfection of myotubes with the AdT viral vector, as detected by triple immunocytochemistry, coupled with BrdU activity, 3 days after induction with

growth medium (GM). (C) Only 2 days in GM, AdT-transfected cells demonstrated reduced staining for the myogenic factors MyoD, myogenin, and MHC but were negative for BrdU. (D) Untransfected (Twist negative) myotubes demonstrated no BrdU activity and expressed normal MyoD, myogenin, and MHC, as expected. (E) Examples of Twist-transfected with active cell cycle (BrdU) and reduced myogenic markers (MyoD, MHC) that underwent cleavage. GAPDH, glyceraldehyde-3-phosphate dehydrogenase; MHC, myosin heavy chain; BrdU, bromodeoxyuridine.

Fig. 4 Twist overexpression targets molecules of muscle cell differentiation and the cell cycle. (A) RT/PCR analysis revealed a substantial reduction at the RNA levels of MyoD in cells transfected with the Twist adenovirus (AdT) compared with the control adenovirus (AdC) and untransfected C2C12 cells. (B) Twist overexpression (AdT) caused reduction at the MyoD protein levels compared with control experiments (C2C12, AdC). (C) Investigation at the RNA levels of cdk4, cyclin D1, and MEF2 after overexpressing the Twist gene (AdT) in differentiated myotubes in comparison with control cells (C2C12, AdC). Twist overexpression caused a substantial increase in the levels of cyclin D1 but did not have significant effect on the cdk4 and MEF2. GAPDH was used as

an internal control. (D) Summary of the RNA quantitation analysis. Values were obtained as ratios of the RNA of interest over the GAPDH internal control. (E) DNA apoptotic assay by ethidium bromide showed no fragmentation in Twist-transduced cells (AdT) and similar necrotic smear to the control-transduced cells (AdC), which was slightly higher to the usual necrosis observed in the C2C12 myotubes. (F) Western blot analysis showed that the caspase-3 levels in Twist-transduced cells (AdT) were similar to those in control-transduced cells (AdC) and untransfected C2C12 cells. GAPDH, glyceraldehyde-3-phosphate dehydrogenase; PCR, polymerase chain reaction.

MyoD seems to play a major role in this since both its RNA and protein levels have been found to be noticeably reduced. Moreover, cell cycle entry control molecule cyclin D1 was shown to be substantially increased in those cells.

Cellular de-differentiation of muscle is not a natural phenomenon observed in mammalian cells. Terminally differentiated mouse myotubes are incapable of re-entering the cell cycle. The above results provide strong evidence that Twist, a transcription factor known to inhibit differentiation of several cell types, can reverse differentiation, re-initiate cell cycle, and cause cleavage of myotubes when overexpressed in differentiated myotubes. This paper provides some insights into the mechanism of Twist-induced myotube de-differentiation too. Following the expression of the exogenous mouse Twist cDNA, a significant number of cells changed morphology, followed by their cleavage.

Immunofluorescence experiments revealed that myogenic factors are reduced upon expression of the adenovirally delivered mouse Twist cDNA in the presence of growth factors. Entry to the cell cycle was observed at a later stage, which was then followed by myotube cleavage.

Molecular analysis performed revealed that MyoD and cyclin D1 were reduced in cells transfected with Twist-adenoviral vector. MyoD is one of the key transcription factors responsible for the differentiation of myoblasts and for inducing myogenesis by regulating the expression of several genes (Wei and Paterson, 2001). It is known that Twist inhibits the action of MyoD, which subsequently inhibits the differentiation of myoblasts into myotubes. This is a known mechanism in which Twist controls muscle cell differentiation (Spicer et al., 1996; Lee et al., 1999; Kophengnavong et al., 2000). Our experiments show that it may well be possible that Twist inhibits MyoD also from this site. Because MyoD is vital during myogenesis, its levels are high when myotubes are formed. Although Twist and MyoD are co-expressed in myoblasts, Twist might be causing a reduction of MyoD as it is overexpressed at a different time than MyoD. As a result there is a retreat in the differentiation, which leads to the structural changes and the reduction in the late and early markers of myogenesis (MHC and myogenin, respectively). MEF2, the partner of MyoD, which exerts effects on the various gene expression targets, was not found reduced. This might imply that Twist inhibits MyoD directly and not indirectly through another pathway. Our experiments also reveal re-activation of the cell cycle, as seen by the DNA synthesis through the BrdU incorporation. This seems to be supported from the substantially increased cyclin D1 levels in cells transfected with the AdT viral vector. Cyclin D1 coupled with the cdk4 form a complex, which then phosphorylates other proteins, thus promoting the initiation of the cycle (Wei and Paterson, 2001). Cdk4 RNA levels were not

found changed in cells transduced with the AdT virus. This was an expected result since cdk4 levels are usually constant during the cell cycle and formation of the cyclinD1/cdk4 complex depends on the availability of cyclin D1. Finally, apoptosis experiments showed that overexpression of the Twist gene does not cause apoptosis in the transduced myotubes (Figs. 4E,4F). Previous reports have demonstrated that Twist might act to prevent apoptosis (Maestro et al., 1999; Hjianioniou et al., 2003; Demontis et al., 2006).

These results point to a mechanism whereby Twist is acting in a pathway by down-regulating the expression of myogenic factors, which usually differentiate terminally myoblasts into myotubes. This in turn gives signal for the re-entry of cells into the cell cycle and their cleavage.

Future experiments will investigate in more detail the specific mechanism by which Twist causes the reversal of differentiation of myotubes in C2C12 and primary cells and also *in vivo*. Finally, the exploitation of the Twist-mediated de-differentiation pathway should provide insights to possible muscle regeneration pathways.

Acknowledgment This work has been supported by the A.G. Leventis Foundation (grant to L. A. P.) and the Cyprus Research Promotion Foundation (grant to L. A. P.).

References

- Andres, V. and Walsh, K. (1996) Myogenin expression, cell cycle withdrawal, and phenotypic differentiation are temporally separable events that precede cell fusion upon myogenesis. *J Cell Biol* 132:657-666.
- Bate, M., Rushton, E. and Currie, D.A. (1991) Cells with persistent twist expression are the embryonic precursors of adult muscles in *Drosophila*. *Development* 113:79-89.
- Demontis, S., Rigo, C., Piccinin, S., Mizzau, M., Sonogo, M., Fabris, M., Brancolini, C. and Maestro, R. (2006) Twist is substrate for caspase cleavage and proteasome-mediated degradation. *Cell Death Differ* 13:335-345.
- Dupont, J., Fernandez, A.M., Glackin, C.A., Helman, L. and LeRoith, D. (2001) Insulin-like growth factor 1 (IGF-1)-induced twist expression is involved in the anti-apoptotic effects of the IGF-1 receptor. *J Biol Chem* 276:26699-26707.
- Echeverri, K. and Tanaka, E.M. (2002) Mechanisms of muscle dedifferentiation during regeneration. *Semin Cell Dev Biol* 13:353-360.
- el Ghouzzi, V., Le Merrer, M., Perrin-Schmitt, F., Lajeunie, E., Benit, P., Renier, D., Bourgeois, P., Bolcato-Bellemin, A.L., Munnich, A. and Bonaventure, J. (1997) Mutations of the TWIST gene in the Saethre-Chotzen syndrome. *Nat Genet* 15:42-46.
- Ephrussi, A., Church, G.M., Tonegawa, S. and Gilbert, W. (1985) B lineage-specific interactions of an immunoglobulin enhancer with cellular factors *in vivo*. *Science* 227:134-140.
- Fuchtbauer, E.M. (1995) Expression of M-twist during postimplantation development of the mouse. *Dev Dyn* 204:316-322.
- Gitelman, I. (1997) Twist protein in mouse embryogenesis. *Dev Biol* 189:205-214.
- Glover, C.P., Bienemann, A.S., Heywood, D.J., Cosgrave, A.S. and Uney, J.B. (2002) Adenoviral-mediated, high-level, cell-specific transgene expression: a SYN1-WPRE cassette mediates increased

- transgene expression with no loss of neuron specificity. *Mol Ther* 5:509–516.
- Hamamori, Y., Wu, H.Y., Sartorelli, V. and Kedes, L. (1997) The basic domain of myogenic basic helix-loop-helix (bHLH) proteins is the novel target for direct inhibition by another bHLH protein, Twist. *Mol Cell Biol* 17:6563–6573.
- Hebrok, M., Wertz, K. and Fuchtbauer, E.M. (1994) M-twist is an inhibitor of muscle differentiation. *Dev Biol* 165:537–544.
- Hjiantoniou, E., Iseki, S., Uney, J.B. and Phylactou, L.A. (2003) DNzyme-mediated cleavage of Twist transcripts and increase in cellular apoptosis. *Biochem Biophys Res Commun* 300:178–181.
- Howard, T.D., Paznekas, W.A., Green, E.D., Chiang, L.C., Ma, N., Ortiz de Luna, R.I., Garcia Delgado, C., Gonzalez-Ramos, M., Kline, A.D. and Jabs, E.W. (1997) Mutations in TWIST, a basic helix-loop-helix transcription factor, in Saethre-Chotzen syndrome. *Nat Genet* 15:36–41.
- Kophengnavong, T., Michnowicz, J.E. and Blackwell, T.K. (2000) Establishment of distinct MyoD, E2A, and twist DNA binding specificities by different basic region-DNA conformations. *Mol Cell Biol* 20:261–272.
- Kumar, A., Velloso, C.P., Imokawa, Y. and Brookes, J.P. (2004) The regenerative plasticity of isolated urodele myofibers and its dependence on MSX1. *PLoS Biol* 2:E218.
- Lee, M.S., Lowe, G.N., Strong, D.D., Wergedal, J.E. and Glackin, C.A. (1999) TWIST, a basic helix-loop-helix transcription factor, can regulate the human osteogenic lineage. *J Cell Biochem* 75:566–577.
- Maestro, R., Dei Tos, A.P., Hamamori, Y., Krasnokutsky, S., Sartorelli, V., Kedes, L., Doglioni, C., Beach, D.H. and Hannon, G.J. (1999) Twist is a potential oncogene that inhibits apoptosis. *Genes Dev* 13:2207–2217.
- McGann, C.J., Odelberg, S.J. and Keating, M.T. (2001) Mammalian myotube dedifferentiation induced by newt regeneration extract. *Proc Natl Acad Sci USA* 98:13699–13704.
- Murray, S.S., Glackin, C.A., Winters, K.A., Gazit, D., Kahn, A.J. and Murray, E.J. (1992) Expression of helix-loop-helix regulatory genes during differentiation of mouse osteoblastic cells. *J Bone Miner Res* 7:1131–1138.
- Murre, C., McCaw, P.S. and Baltimore, D. (1989) A new DNA binding and dimerization motif in immunoglobulin enhancer binding, daughterless, MyoD, and myc proteins. *Cell* 56:777–783.
- Odelberg, S.J., Kollhoff, A. and Keating, M.T. (2000) Dedifferentiation of mammalian myotubes induced by *msx1*. *Cell* 103:1099–1109.
- Poliard, A., Nifuji, A., Lamblin, D., Plee, E., Forest, C. and Kellermann, O. (1995) Controlled conversion of an immortalized mesodermal progenitor cell towards osteogenic, chondrogenic, or adipogenic pathways. *J Cell Biol* 130:1461–1472.
- Riazi, A.M., Lee, H., Hsu, C. and Van Arsdell, G. (2005) CSX/Nkx2.5 modulates differentiation of skeletal myoblasts and promotes differentiation into neuronal cells in vitro. *J Biol Chem* 280:10716–10720.
- Rosania, G.R., Chang, Y.T., Perez, O., Sutherlin, D., Dong, H., Lockhart, D.J. and Schultz, P.G. (2000) Myoseverin, a microtubule-binding molecule with novel cellular effects. *Nat Biotechnol* 18:304–308.
- Sers, C., Emmenegger, U., Husmann, K., Bucher, K., Andres, A.C. and Schafer, R. (1997) Growth-inhibitory activity and downregulation of the class II tumor-suppressor gene H-rv107 in tumor cell lines and experimental tumors. *J Cell Biol* 136:935–944.
- Shiokawa, D., Kobayashi, T. and Tanuma, S. (2002) Involvement of DNase gamma in apoptosis associated with myogenic differentiation of C2C12 cells. *J Biol Chem* 277:31031–31037.
- Spicer, D.B., Rhee, J., Cheung, W.L. and Lassar, A.B. (1996) Inhibition of myogenic bHLH and MEF2 transcription factors by the bHLH protein Twist. *Science* 272:1476–1480.
- Tajbakhsh, S. (2005) Skeletal muscle stem and progenitor cells: reconciling genetics and lineage. *Exp Cell Res* 306:364–372.
- Thisse, B., Stoetzel, C., Gorostiza-Thisse, C. and Perrin-Schmitt, F. (1988) Sequence of the twist gene and nuclear localization of its protein in endomesodermal cells of early *Drosophila* embryos. *Embo J* 7:2175–2183.
- van Doorn, R., Dijkman, R., Vermeer, M.H., Out-Luiting, J.J., van der Raaij-Helmer, E.M., Willemze, R. and Tensen, C.P. (2004) Aberrant expression of the tyrosine kinase receptor EphA4 and the transcription factor twist in Sezary syndrome identified by gene expression analysis. *Cancer Res* 64:5578–5586.
- Wang, X., Ling, M.T., Guan, X.Y., Tsao, S.W., Cheung, H.W., Lee, D.T. and Wong, Y.C. (2004) Identification of a novel function of TWIST, a bHLH protein, in the development of acquired taxol resistance in human cancer cells. *Oncogene* 23:474–482.
- Wei, Q. and Paterson, B.M. (2001) Regulation of MyoD function in the dividing myoblast. *FEBS Lett* 490:171–178.
- Yang, J., Mani, S.A., Donaher, J.L., Ramaswamy, S., Itzykson, R.A., Come, C., Savagner, P., Gitelman, I., Richardson, A. and Weinberg, R.A. (2004) Twist, a master regulator of morphogenesis, plays an essential role in tumor metastasis. *Cell* 117:927–939.

Supplementary material

The following supplementary material is available for this article:

Fig. S1. Efficiency of the Twist antibody on HeLa cells. Twist protein was detected in total (lane 1), nuclear (lane 3), and cytoplasmic (lane 5) extracts from cells transfected with the adenoviral vector (AdT). No Twist was detected in nuclear (lane 2) or cytoplasmic (lane 4) extracts from untransfected cells.

Fig. S2. Quantitative RT/PCR analysis to detect molecular changes in myotubes following their transfection with the Twist gene. Different amounts from the RT were subjected to PCR protocols with a different number of cycles and then plotted in graphs to obtain the linear ranges.

This material is available as part of the online article from: <http://www.blackwell-synergy.com/doi/abs/10.1111/j.1432-0436.2007.00195.x> (This link will take you to the article abstract).

Please note: Blackwell Publishing is not responsible for the content or functionality of any supplementary materials supplied by the authors. Any queries (other than missing material) should be directed to the corresponding author for the article.